Report No. K-TRAN: KSU-15-6 ▪ FINAL REPORT ▪ June 2016

Electrical Resistivity Measurement of Mechanically Stabilized Earth Wall Backfill

Stacey Tucker-Kulesza, Ph.D.
Michael Snapp
Weston Koehn

Kansas State University Transportation Center

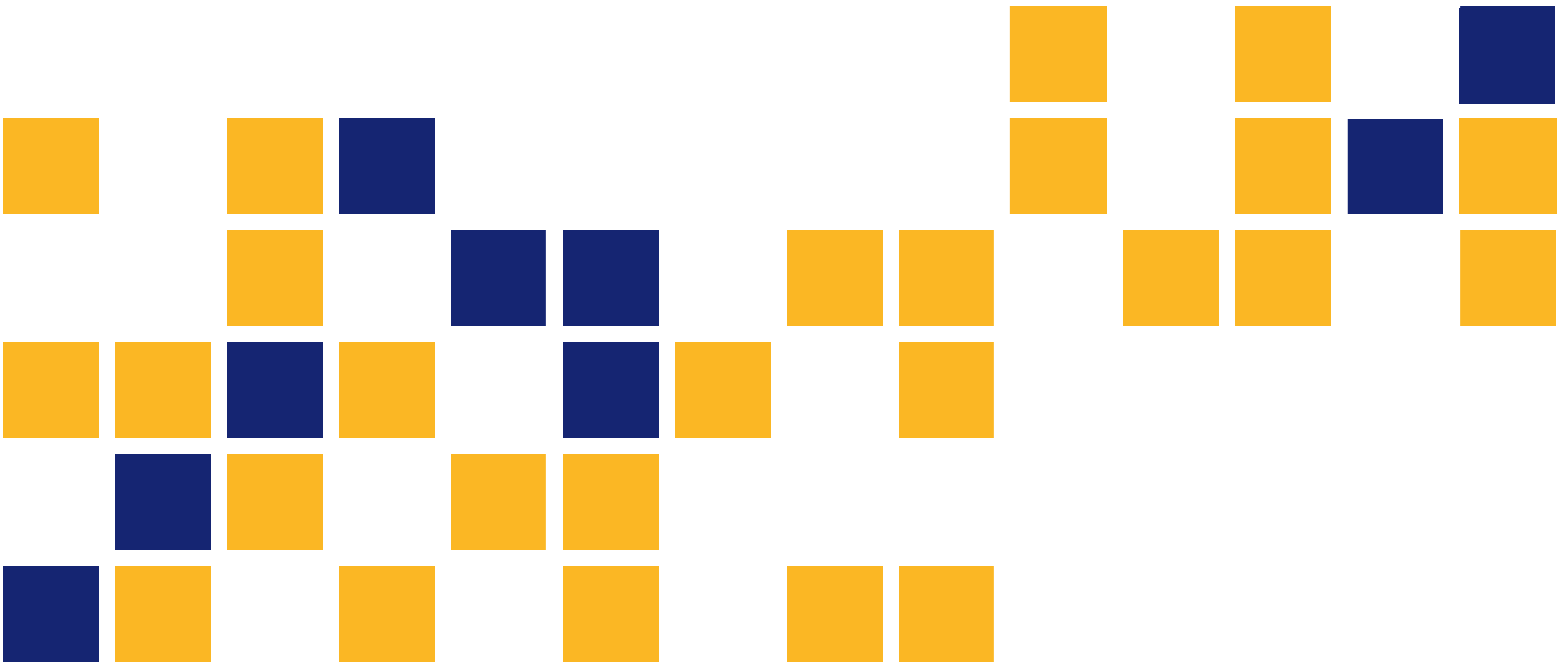

Kansas Department of Transportation

1 Report No. K-TRAN: KSU-15-6	**2 Government Accession No.**	**3 Recipient Catalog No.**
4 Title and Subtitle Electrical Resistivity Measurement of Mechanically Stabilized Earth Wall Backfill		**5 Report Date** June 2016 **6 Performing Organization Code**
7 Author(s) Stacey Tucker-Kulesza, Ph.D., Michael Snapp, Weston Koehn		**7 Performing Organization Report No.**
9 Performing Organization Name and Address Kansas State University Transportation Center Department of Civil Engineering 2122 Fiedler Hall Manhattan, Kansas 66506		**10 Work Unit No. (TRAIS)** **11 Contract or Grant No.** C2032
12 Sponsoring Agency Name and Address Kansas Department of Transportation Bureau of Research 2300 SW Van Buren Topeka, Kansas 66611-1195		**13 Type of Report and Period Covered** Final Report July 2014–March 2016 **14 Sponsoring Agency Code** RE-0657-01
15 Supplementary Notes For more information write to address in block 9.		

In Kansas, mechanically stabilized earth (MSE) retaining walls are typically backfilled with coarse aggregate. Current backfill material testing procedures used by the Kansas Department of Transportation (KDOT) utilize on-site observations for construction quality assurance and the American Association of State Highway and Transportation Officials (AASHTO) Standard T 288-12 (2012), "Standard Method of Test for Determining Minimum Laboratory Soil Resistivity." T 288 is designed to test a soil sample's electrical resistivity, which correlates to its corrosive potential. The test, based on material passing through a No. 10 sieve, is considered inappropriate for coarse aggregates and potentially leads to over-conservative designs. Additionally, T 288 is run on a sample from the aggregate source, but test results may not capture variability of the aggregate used in construction. Electrical resistivity imaging (ERI) provides a two-dimensional (2D) profile of the bulk resistivity of backfill material, thereby reducing uncertainty regarding backfill uniformity as compared to traditional sampling. The objective of this study was to characterize bulk resistivity of in-place MSE wall backfill aggregate using ERI. ERI was used on six walls: five MSE walls and one gravity retaining wall that contained no reinforcement. The ERI field method produced a 2D profile that depicted electrical resistivity uniformity for bulk analysis. A post-processing algorithm was developed to calculate the bulk electrical resistivity of the backfill and reduce the qualitative interpretation of the ERI results. These results indicate that the laboratory analysis of T 288 underestimates the bulk electrical resistivity of in situ backfill material. Recommendations of the study were that ERI surveys and calculated mean electrical resistivity be utilized as construction quality assurance in order to reduce uncertainty of current selection practices.

17 Key Words Mechanically Stabilized Earth Wall Backfill, Electrical Resistivity Imaging, Coarse Aggregate		**18 Distribution Statement** No restrictions. This document is available to the public through the National Technical Information Service www.ntis.gov.	
19 Security Classification (of this report) Unclassified	**20 Security Classification (of this page)** Unclassified	**21 No. of pages** 83	**22 Price**

Form DOT F 1700.7 (8-72)

This page intentionally left blank.

Electrical Resistivity Measurement of Mechanically Stabilized Earth Wall Backfill

Final Report

Prepared by

Stacey Tucker-Kulesza, Ph.D.
Michael Snapp
Weston Koehn

Kansas State University Transportation Center

A Report on Research Sponsored by

THE KANSAS DEPARTMENT OF TRANSPORTATION
TOPEKA, KANSAS

and

KANSAS STATE UNIVERSITY TRANSPORTATION CENTER
MANHATTAN, KANSAS

June 2016

PREFACE

The Kansas Department of Transportation's (KDOT) Kansas Transportation Research and New-Developments (K-TRAN) Research Program funded this research project. It is an ongoing, cooperative and comprehensive research program addressing transportation needs of the state of Kansas utilizing academic and research resources from KDOT, Kansas State University and the University of Kansas. Transportation professionals in KDOT and the universities jointly develop the projects included in the research program.

NOTICE

The authors and the state of Kansas do not endorse products or manufacturers. Trade and manufacturers names appear herein solely because they are considered essential to the object of this report.

This information is available in alternative accessible formats. To obtain an alternative format, contact the Office of Public Affairs, Kansas Department of Transportation, 700 SW Harrison, 2nd Floor – West Wing, Topeka, Kansas 66603-3745 or phone (785) 296-3585 (Voice) (TDD).

DISCLAIMER

The contents of this report reflect the views of the authors who are responsible for the facts and accuracy of the data presented herein. The contents do not necessarily reflect the views or the policies of the state of Kansas. This report does not constitute a standard, specification or regulation.

Abstract

In Kansas, mechanically stabilized earth (MSE) retaining walls are typically backfilled with coarse aggregate. Current backfill material testing procedures used by the Kansas Department of Transportation (KDOT) utilize on-site observations for construction quality assurance and the American Association of State Highway and Transportation Officials (AASHTO) Standard T 288-12 (2012), "Standard Method of Test for Determining Minimum Laboratory Soil Resistivity." T 288 is designed to test a soil sample's electrical resistivity, which correlates to its corrosive potential. The test, based on material passing through a No. 10 sieve, is considered inappropriate for coarse aggregates and potentially leads to over-conservative designs. Additionally, T 288 is run on a sample from the aggregate source, but test results may not capture variability of the aggregate used in construction. Electrical resistivity imaging (ERI) provides a two-dimensional (2D) profile of the bulk resistivity of backfill material, thereby reducing uncertainty regarding backfill uniformity as compared to traditional sampling. The objective of this study was to characterize bulk resistivity of in-place MSE wall backfill aggregate using ERI. ERI was used on six walls: five MSE walls and one gravity retaining wall that contained no reinforcement. The ERI field method produced a 2D profile that depicted electrical resistivity uniformity for bulk analysis. A post-processing algorithm was developed to calculate the bulk electrical resistivity of the backfill and reduce the qualitative interpretation of the ERI results. These results indicate that the laboratory analysis of T 288 underestimates the bulk electrical resistivity of in situ backfill material. Recommendations of the study were that ERI surveys and calculated mean electrical resistivity be utilized as construction quality assurance in order to reduce uncertainty of current selection practices.

Acknowledgements

The authors would like to thank the Kansas Department of Transportation (KDOT) and the Kansas Transportation Research and New-Developments (K-TRAN) Program for funding the research described in this report. The authors thank the KDOT project monitor Jim Brennan and all the construction-site foremen for working with us as we performed testing during their construction. We also thank Dr. Robert Parsons, Dr. Jie Han, and Mr. Zachary Brady at the University of Kansas for providing the laboratory data for this research.

Table of Contents

Abstract i
Acknowledgements ii
Table of Contents iii
List of Tables v
List of Figures vi
Chapter 1: Introduction 1
Chapter 2: Literature Review 5
2.1 American Association of State Highway and Transportation Officials 5
2.2 American Society of Testing and Materials 6
2.3 Federal Highway Administration 6
2.3.1 Soil Corrosion 8
2.3.2 Corrosion Studies of Mechanically Stabilized Earth Retaining Wall Reinforcement 8
2.4 Electrical Resistivity Imaging 10
2.4.1 Four-Electrode Arrays 13
2.4.2 Data Processing 17
Chapter 3: Methodology 20
3.1 Equipment and Software 20
3.2 Preliminary Electrical Resistivity Imaging Data 22
3.2.1 Geosynthetic Wall 1: Interchange of US Route 73 and Interstate 70 22
3.2.2 Geosynthetic Wall 2: Overpass of 118th Street and Interstate 70 25
3.2.3 Geosynthetic Wall 3: South Broadway Street and Centennial Drive 27
3.2.4 Metal Wall 4: Interchange of Ridgeview and Kansas Highway 10 28
3.2.5 Gravity Wall 5: Intersection of Haskell Avenue and East 31st Street 30
3.2.6 Geosynthetic Wall 6: Intersection of 31st St. and Louisiana St. 31
3.3 Partially Saturated Electrical Resistivity Imaging Data 33
3.3.1 Partially Saturated Geosynthetic Wall 2 33
3.3.2 Partially Saturated Metal Wall 4 34
3.3.3 Partially Saturated Gravity Wall 5 35
3.4 Quantitative Post-Processing Algorithm 37
Chapter 4: Electrical Resistivity Results 42
4.1 Geosynthetic Wall 1 42

4.2 Geosynthetic Wall 2 43
4.3 Metal Wall 4 46
4.4 Gravity Wall 5 47
4.5 Geosynthetic Wall 6 49
Chapter 5: Conclusions 51
5.1 Comparison with Brady et al. (2016) Laboratory Electrical Resistivity 56
Chapter 6: Recommendations 57
6.1 Future Work 59
References 60
Appendix A: Preliminary ERI Post Processing 63
Appendix B: Partially Saturated Post Processing 66

List of Tables

Table 1.1: Correlation Between Resistivity Values and Corrosion Potential 3
Table 2.1: Recommended Testing Methods and Standards of MSE Wall Backfill Material 7
Table 2.2: Resistivity of Common Geological Materials 10
Table 3.1: Characteristics of GW1 614 23
Table 3.2: Characteristics of GW1 714 24
Table 3.3: Characteristics of GW2 614 26
Table 3.4: Characteristics of GW3 714 27
Table 3.5: Characteristics of MW4 914 29
Table 3.6: Characteristics of GRW5 215 31
Table 3.7: Characteristics of GW6 615 32
Table 3.8: Characteristics of SGW2 515 33
Table 3.9: Characteristics of SMW4 1014 35
Table 3.10: Characteristics of SGR5 515 36
Table 3.11: Norm of Residuals from the Normal Distribution of Normal and Lognormal CDFs 39
Table 5.1: Summary of Bulk Electrical Resistivity Testing Results 51
Table 6.1: Corrosion Potential Using ERI 58

List of Figures

Figure 1.1: Typical MSE Wall Attributes 1
Figure 2.1: General Configuration of Current and Potential Electrodes 11
Figure 2.2: Apparent Electrical Resistivity Pseudosection of the Dipole-Dipole Array 13
Figure 2.3: 2D Apparent Electrical Resistivity Pseudosection from Field Data 13
Figure 2.4: Electrode Geometric Configuration of the Dipole-Dipole Array 14
Figure 2.5: Electrode Geometric Configuration of the Wenner Array 15
Figure 2.6: Electrode Geometric Configuration of the Schlumberger Array 16
Figure 2.7: Electrode Geometric Configuration of the Inverse Schlumberger Array 16
Figure 2.8: Beginning of the Computer Modeling and Inversion 19
Figure 3.1: Equipment (a) Stainless Steel Electrode Setup; (b) Equipment Setup in the Field 21
Figure 3.2: Correlation of Average Injected Current and Average Contact Resistance 22
Figure 3.3: GW1 Experimental Setup (a) June 18, 2014; (b) July 9, 2014 23
Figure 3.4: GW1 614 Inverted Resistivity Profile 24
Figure 3.5: GW1 714 Inverted Resistivity Profile 25
Figure 3.6: GW2 Experimental Setup 25
Figure 3.7: GW2 614 Inverted Resistivity Profile 26
Figure 3.8: GW3 714 Inverted Resistivity Profile 28
Figure 3.9: MW4 Experimental Setup 28
Figure 3.10: MW4 914 Inverted Resistivity Profile 30
Figure 3.11: GRW5 Experimental Setup 30
Figure 3.12: GRW5 215 Inverted Resistivity Profile 31
Figure 3.13: GW6 Experimental Setup 32
Figure 3.14: GW6 615 Inverted Resistivity Profile 33
Figure 3.15: SGW2 Experimental Setup 34
Figure 3.16: SGW2 515 Inverted Resistivity Profile 34
Figure 3.17: SMW4 1014 Inverted Resistivity Profile 35
Figure 3.18: SGR5 515 Inverted Resistivity Profile 36
Figure 3.19: Histogram of GW1 614 37
Figure 3.20: PDF of GW1 614 40
Figure 4.1: GW1 Final Inverted Resistivity Section 42
Figure 4.2: GW1 Final (a) Histogram; (b) PDF 43

Figure 4.3: GW2 Final Inverted Resistivity Section 44
Figure 4.4: GW2 Final (a) Histogram; (b) PDF 44
Figure 4.5: GW2 (a) GW2 Final Inverted Resistivity Section; (b) GW2 614 45
Figure 4.6: MW4 Final Inverted Resistivity Section 46
Figure 4.7: MW4 Final (a) Histogram; (b) PDF 47
Figure 4.8: GRW5 415 Final Inverted Resistivity Section 48
Figure 4.9: GRW5 Final (a) Histogram; (b) PDF 48
Figure 4.10: GW6 Final Inverted Resistivity Section 49
Figure 4.11: GW6 Final (a) Histogram; (b) PDF 50
Figure 5.1: Summary of Measured Bulk Resistivity 53
Figure 5.2: Grain Size Distributions of Samples from MSE Walls 53
Figure 5.3: Dry and Partially Saturated Survey Bulk Resistivity 55
Figure A.1: GW2 Histogram 63
Figure A.2: GW2 PDF 63
Figure A.3: MW4 Histogram 64
Figure A.4: MW4 PDF 64
Figure A.5: GRW5 Histogram 65
Figure A.6: GRW5 PDF 65
Figure B.1: SGW2 Histogram 66
Figure B.2: SGW2 PDF 66
Figure B.3: SMW4 Histogram 67
Figure B.4: SMW4 PDF 67
Figure B.5: SGR5 Histogram 68
Figure B.6: SGR5 PDF 68

This page intentionally left blank.

Chapter 1: Introduction

The Kansas Department of Transportation (KDOT) utilizes mechanically stabilized earth (MSE) retaining walls throughout the Kansas highway system. MSE walls were first implemented in the United States in the 1970s due to their cost efficiency and strength (Armour, Bickford, & Pfister, 2004). MSE walls generally consist of three components: vertical facing, leveling pad, and reinforced backfill (Figure 1.1). Reinforcement extends from the vertical facing of the wall into the backfilled soil, advantageously utilizing the soil's strength properties and weight to support the wall.

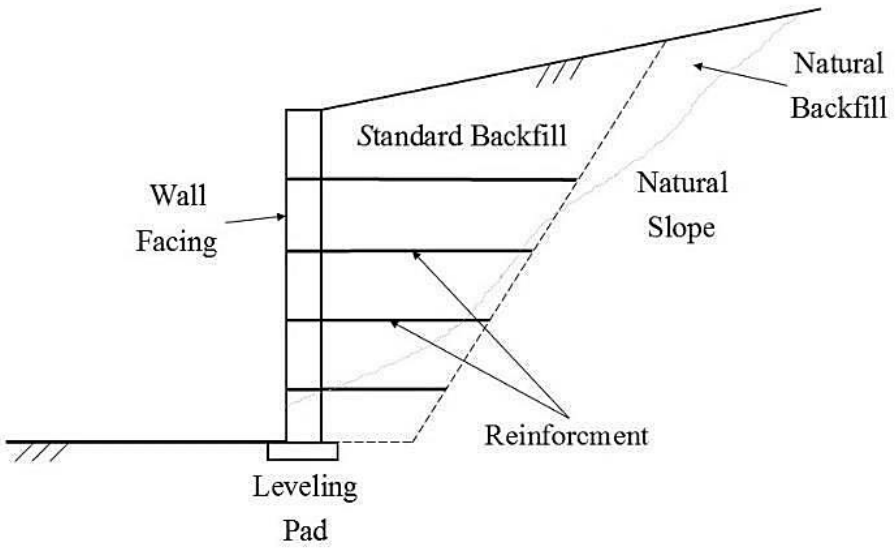

Figure 1.1: Typical MSE Wall Attributes

Backfill is selected prior to construction based on specific material properties, such as its potential to foster a corrosive environment. MSE walls use either metallic or polymeric materials as reinforcement. One primary disadvantage of metal reinforcement is that it is susceptible to corrosion. Corrosion, the process of metal material returning to its stable natural state, is caused by naturally occurring electric current flowing between two metal objects or two points on the same material when an electrolyte (typically water) is present in the soil (Elias, Fishman,

Christopher, & Berg, 2009). Corrosion of the reinforcement can result in loss of thickness, stiffness, and strength. In extreme cases, reinforcement corrosion can lead to failure of the MSE-wall system (Armour et al., 2004; Thornley & Siddharthan, 2010). Although polymeric reinforcement, such as geosynthetics, is not susceptible to corrosion, typically all backfill material must satisfy corrosion criteria in transportation structures.

Assessment of a soil's corrosive potential requires accurate evaluation of pH, electrical resistivity, and sulfate and chloride concentrations of fluids in contact with the soil. The American Association of State Highway and Transportation Officials (AASHTO) has specified rates of reinforcement corrosion and developed a standard test method used to determine a soil's corrosion potential. In addition, AASHTO, the American Society for Testing Materials (ASTM), the Federal Highway Administration (FHWA), and state Departments of Transportation (DOTs) have created guidelines and standards for construction of MSE walls, along with testing procedures and construction quality assurance (CQA) practices. This study focused on a CQA test to complement the AASHTO Standard T 288-12 (2012), "Standard Method of Test for Determining Minimum Laboratory Soil Resistivity," which is used to determine corrosion potential of soils.

AASHTO Standard T 288 utilizes a sample of soil gathered from the selected backfill material which passes through a No. 10 sieve (2.00 mm). Water is added to the material passing the sieve and then placed into a 688-cm3 box. A meter is attached to the box and the resistance of the soil is measured. The sample is then removed, more water is added, and then tested again and repeated until a minimum resistance is measured. The resistivity is calculated by multiplying the resistance by a constant for the box which is derived from the relationship of the surface area of one electrode and the distance between the two electrodes. FHWA has established qualitative levels of corrosiveness with measured ranges of electrical resistivity, as shown in Table 1.1. Select backfills identified as moderate to mildly corrosive are generally acceptable for MSE walls.

The T 288 method has many disadvantages. The coarse aggregate used for MSE walls often contains only a small percentage of material that passes the No. 10 sieve. Thapalia, Borrok, Nazarian, and Garibay (2011) found that the small percentage of material that passes the No. 10

sieve is typically not representative of the corrosive nature of the aggregate, potentially leading to unnecessary rejection of the material. An additional disadvantage of T 288, as with all sampling methods, is that it provides only point sources of information, often from a stockpile that represents potential sources of fill material. This study investigated the application of electrical resistivity imaging (ERI) as an in situ measurement for corrosion potential of aggregate by determining the bulk electrical resistivity of the aggregate.

Table 1.1: Correlation Between Resistivity Values and Corrosion Potential

Aggressiveness	Resistivity (Ωcm)
Very corrosive	< 700
Corrosive	700 to 2,000
Moderately corrosive	2,000 to 5,000
Mildly corrosive	5,000 to 10,000
Noncorrosive	> 10,000

Note: Adapted from Elias et al. (2009)

The only common field method used to predict and monitor reinforcement corrosion is the addition of metal coupons (Elias et al., 2009). Coupons are small samples of metal reinforcement that are inserted near the face of the wall during construction and then removed for degradation testing. Their removal does not affect the integrity of the MSE wall and sample degradation is attributed to corrosion. Currently, there is a need for an in situ testing method that can be used in concert with T 288 to determine the corrosion potential of MSE wall backfill. The ERI in the field can provide results of the entire wall and be performed on the aggregates in situ without material being crushed or saturated, which is more indicative of MSE wall backfill.

This study investigated the application of ERI, a near-surface nondestructive geophysical field testing method used to determine the bulk electrical resistivity of MSE wall backfill. Few known in situ testing procedures exist for determining electrical resistivity of aggregate backfill. ERI provides a two-dimensional (2D) profile of subsurface electrical resistivity distribution, thereby providing more information than a sample tested in a laboratory setting. In this study, ERI was applied to five MSE walls specified by KDOT: four walls that contained geosynthetic reinforcement and one wall that had metallic reinforcement. A sixth wall that contained no

reinforcement was also tested. A quantitative post-processing algorithm was developed to determine bulk electrical resistivity of in-place backfill.

This report is divided into six chapters. The literature review is included in Chapter 2 following this introduction. Chapter 3 discusses equipment used during testing, the ERI field testing procedure, the preliminary results of each wall, and the quantitative post-processing. Chapter 4 presents the final bulk electrical resistivity of the structures. Finally, conclusions are presented in Chapter 5 and recommendations and future work are presented in Chapter 6.

Chapter 2: Literature Review

AASHTO, ASTM, FHWA, and state DOTs have developed guidelines, standards, testing procedures, and CQA practices for retaining wall backfill materials. Current MSE wall construction testing and practices are primarily laboratory analyses with limited in situ investigation.

2.1 American Association of State Highway and Transportation Officials

AASHTO has developed and published specifications and testing (field and laboratory) procedures primarily to be used in transportation infrastructure construction. AASHTO has developed a test that may be used for MSE wall backfill (AASHTO Standard T 288-12, 2012). In addition to AASHTO Standard T 288-12 and other applicable test procedures, AASHTO has also published specifications and guidelines for MSE retaining wall construction.

AASHTO Standard T 288-12 determines electrical resistivity of a soil sample which is an indicator of its corrosion potential. The test can also identity the soil conditions that may accelerate metal corrosion in an MSE wall or underground metallic elements. It involves gathering a sample from the borrow material and determining minimum soil resistivity through laboratory testing. The sample is pulverized to pass a 2-mm sieve (No. 10) and mixed with distilled water. After the soil has been cured for 12 hours, it is remixed thoroughly and compacted into layers in a soil box (two box sizes outlined in the standard). The soil box contains two electrodes at opposite ends that are connected to a resistivity meter. Resistance is measured between the two electrodes and soil resistivity is calculated. After the test is completed, the soil is removed, water is added to the soil, remixed, placed back into the box, and another measurement is taken. Measurements are repeated until a minimum soil resistivity value is obtained. The relationship of resistivity and corrosion is discussed in Section 2.3.1. AASHTO is a major implementer of CQA practices and testing procedures, but there is still a need for in situ testing methods.

2.2 American Society of Testing and Materials

ASTM has also produced standards and specifications, such as ASTM G187-12a (2012), "Standard Test Method for Measurement of Soil Resistivity Using the Two-Electrode Soil Box Method." This test determines soil resistivity to predict corrosion potential and is a laboratory analysis method that is commonly paired with the in situ test method ASTM G57-06 (2006), "Standard Test Method for Field Measurement of Soil Resistivity Using the Wenner Four-Electrode Method."

ASTM Standard Test G187-12a is similar to the AASHTO Standard T 288-12 test in that it requires a soil sample to be wetted and placed in a box of specific dimensions outlined in the standard with the ability to connect a resistivity meter. Water is added, the soil is remixed, and resistance is again measured until a minimum measurement is recorded. The ASTM standard does not require material sieving nor directly comment on soil types appropriate for testing. The only recommendation mentioned for the test sample is the removal of "foreign material such as gravel, small stones, roots, twigs, and so forth," possibly implying that the testing method is not suitable for coarse aggregate backfill material (ASTM G187-12a, 2012).

ASTM has also published ASTM G57-06 (2006), "Standard Test Method for Field Measurement of Soil Resistivity Using the Wenner Four-Electrode Method." This test method measures soil resistivity to determine the expected corrosion rate and design protection of buried structures. This test method is one of the few in situ testing methods for soil corrosion, but provides no information in regards to its use on MSE wall backfill or its use in coarse aggregate material. Similar to AASHTO, no in situ testing methods currently exist specifically for coarse backfill material of an MSE wall.

2.3 Federal Highway Administration

FHWA has developed many detailed standards and guidelines that outline construction of MSE walls, including documents such as "Design of Mechanically Stabilized Earth Walls and Reinforced Soil Slopes" Volumes I and II (Berg, Christopher, & Samtani, 2009a, 2009b) and "Corrosion/Degradation of Soil Reinforcements for Mechanically Stabilized Earth Walls and Reinforced Soil Slopes" (Elias et al., 2009; see also FHWA, 2015). These documents provide

information regarding the design process and construction practices of MSE walls. Elias et al. (2009) describe methods that may be used to prevent corrosion and outlines testing methods and specifications that should be considered for MSE wall construction. The report recommends specific backfill material properties when using metal reinforcement, as shown in Table 2.1.

Table 2.1: Recommended Testing Methods and Standards of MSE Wall Backfill Material

Attribute	Recommended Value	Test Method
Electrical Resistivity	> 3,000 Ohm-cm*	AASHTO T 288
pH	5 to 10	AASHTO T 289
Organic Content	Max 1%	AASHTO T 267
Chlorides	< 100 PPM	ASTM D4327
Sulfates	< 200 PPM	ASTM D4327

Source: Elias et al. (2009)

FHWA also provides monitoring methods for metal reinforced MSE walls. One method is the retrieval of coupons. These coupons, which are reinforcement materials placed during construction with access during post-construction, are removed and analyzed for degradation (Elias et al., 2009). Their degradation relates to the corrosion within the wall. However, removal of coupons does not affect the stability of the wall. This method requires installation during construction to monitor the wall.

As discussed, limited in situ testing procedures and laboratory methods currently exist for backfill material of an MSE wall. AASHTO Standard T 288-12 (2012) requires using the minimum soil electrical resistivity value obtained once the sample becomes a slurry mix from the addition of water. This is not indicative of materials used in MSE walls constructed by KDOT as most are constructed with free-draining coarse aggregates; water is typically not present. T 288 also requires the material to pass through a No 10. (2 mm) sieve, essentially excluding coarse aggregates.

2.3.1 Soil Corrosion

Reinforcement of MSE walls can either be metal or geosynthetic material. Metal is used at times because it is less expensive than geosynthetics. However, metal is a corrosive material and this has caused the failure of many MSE walls. Recent advancements of geosynthetics have decreased the use of metals as MSE wall reinforcement. Despite the lack of corrosion potential in geosynthetics, many agencies still prefer metal reinforcement. Corrosion is the degradation of metals through environmental electrochemical reactions and is the process of the metals returning to their natural state. Moisture that penetrates the soil typically contains dissolved compounds, resulting in an acidic environment and providing an electrolyte in the soil. The presence of these electrolytes causes voltage differences between the metal and the soil and allows natural current to flow between the two materials. The current flows from the anode (metal) to the cathode (soil and electrolyte) and back again to the anode, completing the circuit. Due to the loss of metal ions to the electrolyte, the metal becomes corroded (Elias et al., 2009).

Tests discussed in the previous sections require soil material to be tested for resistivity. As stated in the ASTM Standard G187-12a (2012), high resistivity values of soil typically result in a low corrosive environment, while low resistivity values are typically indicative of a highly corrosive environment. Lower resistivity values, indicative of finer-grained material, correlate to higher corrosive values typically due to the increase of particle contact, allowing for the flow of current and also the retention of water, the electrolyte. Table 1.1 showed the range of resistivity values for potential corrosion.

2.3.2 Corrosion Studies of Mechanically Stabilized Earth Retaining Wall Reinforcement

Many studies have investigated corrosion of metal reinforcement of MSE walls prior to complete catastrophic wall failure. A case study in Nevada examined preexisting MSE wall reinforcements thought to have been affected by corrosion. The reinforcement corrosion was accidentally discovered in two MSE walls, leading to uncertainty regarding the remaining MSE walls within the State of Nevada. Corrosion of the reinforcement of one wall was found during construction of an additional sound-wall above the preexisting wall. The corrosion of the

reinforcement of the second wall was found during demolition of a small portion of the wall for an expansion project (Thornley & Siddharthan, 2010).

Reinforcement and backfill samples were taken directly from the walls and tested. Both walls were well documented during construction, and each wall had test results for the Nevada test method. This test measures conductivity of water from a saturated soil solution with reinforced fill, which is different from the AASHTO T 288 test. Statistical analysis of metal loss was performed on the corroded reinforcement based on the original diameters. Test results showed that the Nevada T-235B (which classified the material as only moderately corrosive) underestimated the corrosion potential of the backfill material compared to AASHTO T 288 (which classified the material as highly corrosive). A statistical analysis of the corrosion and also a model used to determine the behavior of the MSE wall under static and seismic loading conditions showed results that the walls were unable to retain stability for the designed life of 75 years (Thornley & Siddharthan, 2010).

In 2002, six panels failed at the base of a MSE wall designed and constructed in 1978 (Armour et al., 2004). The wall was part of an overpass structure over a railroad in Soda Springs, Idaho. Upon visual inspection, the metal reinforcement was determined to have experienced severe corrosion, thereby causing the failure. Reinforcement strength decreased from the degradation, causing panels to detach from the face of the wall. Due to unstable conditions caused by the initial failure, additional panels began to fail, ending when the surrounding reinforcement formed an arch-shaped support and the failure was stabilized. Approximately 530 ft^3 (15 m^3) of material fell from the wall. Laboratory testing was performed on the backfill materials to determine the reason for the accelerated corrosion rate of the reinforcement. According to AASHTO standards and the Idaho Department of Transportation standards, the backfill material was classified as very corrosive. Remediation of the MSE wall consisted of the installation of soldier piles, rock anchors, and reinforced shotcrete pilasters at each soldier pile in order to support the wall.

As seen in these case studies, reinforcement corrosion is a concern when constructing an MSE wall. Many testing procedures may be utilized to prevent these failures, but the majority of

testing procedures are laboratory-based. Visual inspections and engineering judgment are the only known field methods currently used for MSE wall construction quality assurance practices.

2.4 Electrical Resistivity Imaging

ERI, developed in the early 1900s, is a near-surface geophysical, non-destructive testing method currently used in various fields due to the availability of equipment, ease of setup, procedure, and interpretation (Lowrie, 2007). ERI has applications in fields such as archaeology, geology, environmental, geotechnical, and construction, with applications in these fields including hydrogeological contamination mapping (Vaudelet et al., 2011), geological subsurface site characterization (Chambers et al., 2013), environmental landfill studies (Bernstone, Dahlin, Ohlsson, & Hogland, 2000), monitoring of soil moisture content (Zhou, Shimada, & Sato, 2001), and geotechnical site investigations to determine depth of bridge foundations (Arjwech et al., 2013).

Table 2.2: Resistivity of Common Geological Materials

Material	Resistivity (Ωm)
Clay	1- 20
Sand, wet to moist	20- 200
Shale	1- 500
Porous limestone	100- 10^3
Dense limestone	10^3- 10^6
Metamorphic rocks	50- 10^6
Igneous rocks	10^2- 10^6

Source: Everett (2013)

Subsurface characteristics such as water content and saturation, porosity, permeability, mineralogy, clay content, and temperature affect electrical resistivity measurements (Zonge, Wynn, & Urquhart, 2005). Typical electrical resistivity values of common geological materials are outlined in Table 2.2. Electrical resistivity of a soil tends to decrease with increased water content and saturation (Bai, Kong, & Guo, 2013). Materials with high clay content and metallic minerals tend to have low electrical resistivity because the clay and metallic minerals are

conductive, allowing the flow of current to easily pass through the material. Electrical resistivity typically decreases with decreased porosity due to the decrease in void space between particles that prohibit current flow.

Electrical resistivity, an intrinsic material property, defines a material's ability to resist or oppose the flow of electric current. Resistivity (ρ) is represented in units of Ohm meter (Ωm) and is the inverse of conductivity (σ). In an ERI survey, direct electric current is injected into the subsurface and voltage is measured across two electrodes. The voltage potential measured across the Electrodes C and D of the voltmeter in Figure 2.1 due to the current source, I, is the difference:

$$V_{CD} = V_C - V_D = \frac{\rho I}{2\pi}\left(\frac{1}{r_{AC}} - \frac{1}{r_{AD}}\right)$$

Equation 2.1

Where:

r_{AC} and r_{AD} are the distance from the current source to the voltage potential electrode.

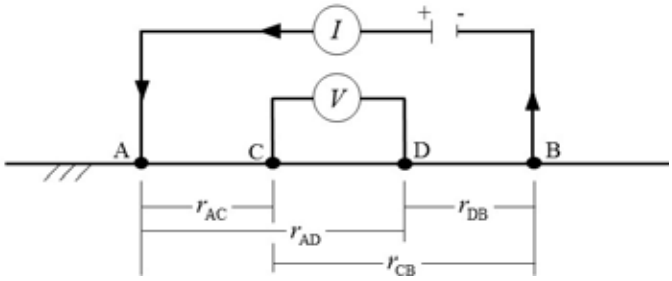

Figure 2.1: General Configuration of Current and Potential Electrodes

Equation 2.1 assumes that the subsurface is a uniform homogenous material with uniform resistivity. In reality, the resistivity of the earth is heterogeneous; therefore, Equation 2.1 is rearranged to solve for apparent resistivity, ρ_a, which is the resistivity that would be measured if in fact the earth were homogenous:

$$\rho_a = \frac{2\pi V_{CD}}{I}\left[\frac{1}{r_{AC}} - \frac{1}{r_{AD}}\right]^{-1}$$

Equation 2.2

As shown in Figure 2.1, ERI surveys include both a point source and return point sink of current so that Equation 2.2 is:

$$r_a = \frac{2\pi V}{I}\left[\frac{1}{r_{AC}} - \frac{1}{r_{CB}} - \frac{1}{r_{AD}} + \frac{1}{r_{DB}}\right]^{-1}$$

Equation 2.3

When running an ERI survey, a known electric current (*I*) is injected into the subsurface and the corresponding voltage potential (*V*) is measured at known distances (*r*) so that the apparent resistivity can be calculated.

Forward modeling and inversion are used to determine the electrical resistivity of the subsurface. Apparent electrical resistivity data are typically plotted into a two-dimensional (2D) profile, or pseudosection. For ease of plotting, the convention is to locate the subsurface point at the intersection of lines that extend from the center of the two pairs of electrodes (current and potential), 45° from the ground surface, as shown in Figure 2.2 (Hallof, 1957). This method is repeated for each pair of electrodes, thereby generating a pseudosection of apparent electrical resistivity, as shown in Figure 2.3. The geometry of the electrode setup, subsurface material, and electrode spacing slightly alter the depth of ERI investigations (Edwards, 1977; Loke, 1999).

The traditional method of four electrodes has been modernized into an automated system in which multiple electrodes are connected, thereby increasing the effectiveness and efficiency of ERI. Multiple electrodes are attached to a data acquisition system that runs a desired command file. The command file contains information on the spacing of the electrodes and the field geometry. From this information, the system relays which electrodes to use as current and potential. Depending on the system, multiple potential readings may be taken per current electrode pair. This allows the process to optimize testing efficiency, decreasing testing time.

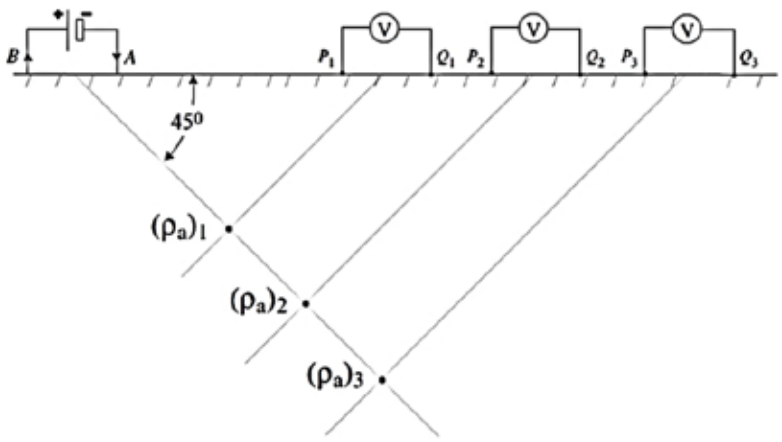

Figure 2.2: Apparent Electrical Resistivity Pseudosection of the Dipole-Dipole Array
Source: Tucker, Briaud, Hurlebaus, Everett, and Arjwech (2015)

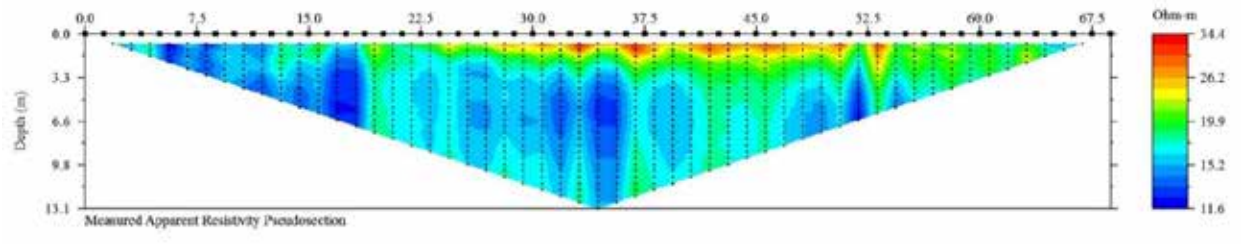

Figure 2.3: 2D Apparent Electrical Resistivity Pseudosection from Field Data

2.4.1 Four-Electrode Arrays

An array defines the current and potential electrode configurations used during testing. Three main arrays are used in ERI: dipole-dipole, Wenner, and Schlumberger. Each test differs according to electrode configuration or spacing and each has unique advantages and disadvantages. When planning a survey, the necessary depth to image the medium of interest and the required resolution are the main considerations. In general, as electrode spacing increases, depth of signal penetration increases, and when spacing decreases, depth of signal penetration decreases (Furman, Ferré, & Warrick, 2003); however, there is a trade-off in resolution.

Three areas of concern when comparing and choosing an array include signal-to-noise ratio, electromagnetic coupling (EM), and resolution (vertical and horizontal). Signal-to-noise ratio refers to the ratio of the desired signal to the background noise. EM, also known as cross-

wire coupling, is the interference between the transmitter and receiver wires (Zonge et al., 2005). Vertical resolution refers to the ability of the array to provide data with depth, and horizontal resolution refers to the ability to gather data laterally along the survey line. The following sections describe each array and present a pictorial representation of the configuration, the apparent resistivity equation with geometric spacing, and advantages and disadvantages of each array.

2.4.1.1 Dipole-Dipole Array

The dipole-dipole array consists of the current pair of electrodes and the potential pair of electrodes spaced equal distance, *a*, separated by a factor of na (Figure 2.4). Equation 2.3 can be simplified using the spacing of the dipole-dipole array:

$$r_a = \pi an(n+1)(n+2)\frac{V}{I} \qquad \textbf{Equation 2.4}$$

Where:

a is electrode spacing,

n times a spacing represents spacing of the electrode pairs,

I is input current, and

V is measured voltage.

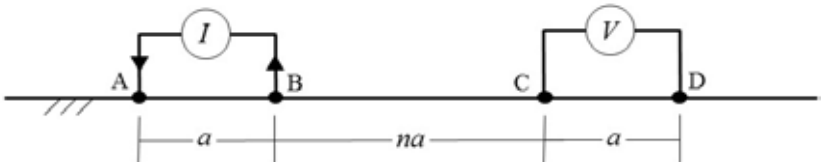

Figure 2.4: Electrode Geometric Configuration of the Dipole-Dipole Array

The dipole-dipole array provides good lateral and vertical resolutions with minimal EM coupling (Zonge et al., 2005). This array was initially utilized in the study, but due to the increased time to run a survey, it was ultimately not selected as the optimal array. The dipole-dipole array requires approximately 40 minutes utilizing a 56 electrode and 1.2 seconds between measurements.

2.4.1.2 Wenner Array

Spacing of the Wenner array, as shown in Figure 2.5, is set to equal distance a between electrodes, allowing the greatest lateral resolution compared to dipole-dipole and Schlumberger arrays (Zonge et al., 2005). Unfortunately, this geometric arrangement limits overall survey depth and increases EM coupling (Stummer, Maurer, & Green, 2004). The apparent electrical resistivity with Wenner array geometric spacing is:

$$r_a = 2\pi a \frac{V}{I}$$

Equation 2.5

Testing time for a 56 electrode setup is the longest of the three arrays, requiring over an hour. This array was not used in this study due to the amount of time the test takes and lack of resolution with depth.

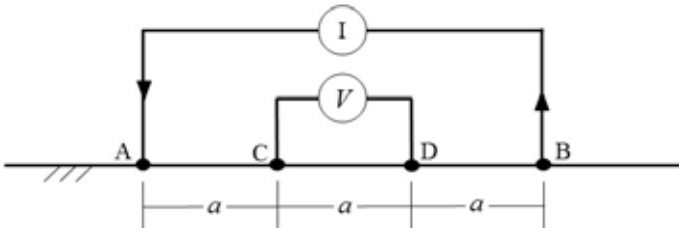

Figure 2.5: Electrode Geometric Configuration of the Wenner Array

2.4.1.3 Schlumberger

The traditional four electrode geometric configuration of the Schlumberger array consists of potential electrodes located inside current electrodes (Figure 2.6). Electrode arrangement is symmetrical about the center of the test setup. Potential electrodes are spaced at distance a from the center and current electrodes are spaced at distance na. The apparent resistivity using the specific electrode spacing of the Schlumberger array is:

$$r_a = \frac{1}{2}\pi a(n-1)(n+1)\frac{V}{I}$$

Equation 2.6

The Schlumberger array provides the best vertical resolution of the three arrays with low signal-to-noise ratio (Stummer et al., 2004). However, the Schlumberger array provides poor lateral resolution and high EM coupling (Zonge et al., 2005). This array requires approximately 1 hour for a 56 electrode test.

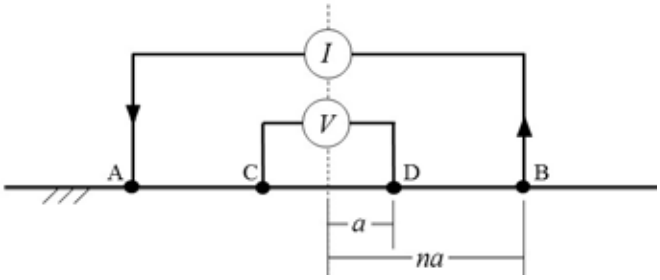

Figure 2.6: Electrode Geometric Configuration of the Schlumberger Array

2.4.1.4 Inverse Schlumberger

The inverse Schlumberger array switches the inner potential electrodes with current electrodes and outer current electrodes with potential electrodes while maintaining spacing configuration of the Schlumberger array (Figure 2.7). The setup of current and potential electrodes previously mentioned allows multiple potential electrodes to be used per current pairs in the automated system, speeding up testing time from 1 hour in the Schlumberger array to 32 minutes for a 56 electrode test. The inverse Schlumberger array was primarily utilized in this study because of its relatively fast testing time and optimum data acquisition with good depth resolution.

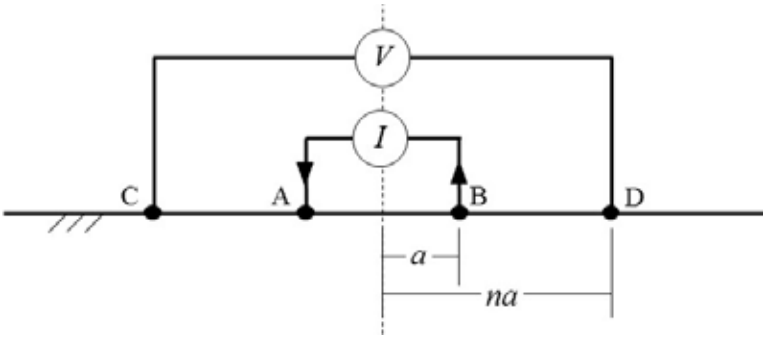

Figure 2.7: Electrode Geometric Configuration of the Inverse Schlumberger Array

2.4.2 Data Processing

Forward modeling and data inversion are used to convert apparent electrical resistivity measured in the field into inverted electrical resistivity used for interpretation. Advanced Geosciences Inc. (AGI) commercial software EarthImager 2D was used exclusively for this research (AGI, 2007). EarthImager initially graphically displays the measured apparent electrical resistivity pseudosection (Figure 2.8a) from field testing. Major spikes in measured data, negative values, maximum and minimum apparent resistivity values, and minimum voltage may be removed at this time. First, a forward model is calculated utilizing the 2D electric potential of the subsurface,

$$\frac{\partial}{\partial x}\left(\sigma \frac{\partial V}{\partial x}\right)+\frac{\partial}{\partial z}\left(\sigma \frac{\partial V}{\partial z}\right)- k^2 \sigma V = - I \times \delta(x) \times \delta(z) \qquad \textbf{Equation 2.7}$$

Where:

V is scalar electrical potential,

I is electric current source,

k is wavenumber, and

σ is electrical conductivity as a function of (x, z) (AGI, 2007).

Finite element modeling was used with four elements between each electrode. The partial differential equation is used to estimate the potential at each element. The starting model for Equation 2.7 is the average of all measured apparent resistivity data (Figure 2.8c).

Once the forward model is created, the data misfit between the field data and the calculated data is determined. The objective in this process is to determine the resistivity model (predicted data) which best fits the measured field data. The root mean squared (RMS) error is one of the parameters that provides insight on data misfit. RMS is:

$$RMS = \sqrt{\frac{\sum_{i=1}^{n} \left(\frac{d_i^{Pred} - d_i^{Meas}}{d_i^{Meas}} \right)^2}{N}} \cdot 100\%$$

Equation 2.8

Where:

N is the total measurements,

d_i^{pred} is predicted data, and

d_i^{meas} is the measured data.

In general, an RMS of less the 5% is desired, between 5% and 10% is acceptable, and greater than 10% is unacceptable and may be a misrepresentation of the true subsurface distribution. The L2-Norm is a weighted data misfit which is a key part of the objective function to be minimized during inversion. The L2-Norm is normalized by the number of measurements so that:

$$\text{L2-Norm} = \frac{\sum_{i=1}^{N} \left(\frac{d_i^{pred} - d_i^{meas}}{W_i} \right)^2}{N}$$

Equation 2.9

Where:

W_i is the data weight of estimated noise and all other variables have previously been defined.

Convergence of the model is achieved when the L2-Norm is equal to or less than unity. Next a smooth model inversion, commonly referred to as Occam's inversion, is utilized to invert the data. Smooth model inversion determines the smoothest model in which the model and data fit to an a-priori Chi-squared statistic (estimated noise). The data are inverted and then compared to the stop criteria. The stop criteria are based on a number of iterations, RMS, and L2-Norm. The modeling and inversion are completed after any of the stop criteria are reached. The RMS and L2-Norm are used during inversion in two ways. Primarily, by iterating until both an acceptable RMS and L2-Norm are achieved, the uncertainty of the subsurface model is reduced. Additionally because both RMS and L2-Norm are a function of the estimated data noise, they

can be used as an indicator of the appropriateness of the predicted noise. For example, if the noise estimate is too low, the iteration may continue until the RMS is less than the anticipated noise, however the L2-Norm will not converge. By having both an RMS less than 5% and an L2-Norm less than 1.0, inherent non-uniqueness and uncertainty of the model is reduced.

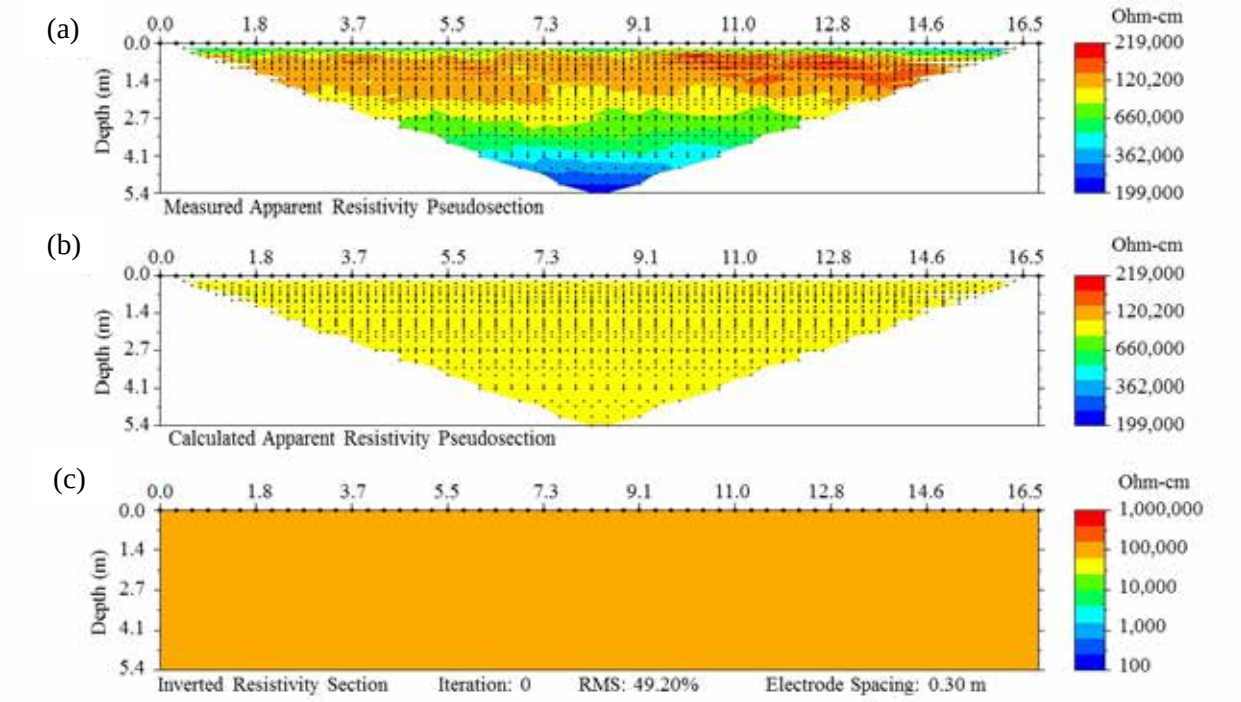

Figure 2.8: Beginning of the Computer Modeling and Inversion

Once inversion and model settings are established, the model and inversion process can begin. The forward model and inversion process are performed by comparing the measured apparent resistivity pseudosection (Figure 2.8a) to the calculated apparent resistivity pseudosection (Figure 2.8b). The inverted resistivity section is determined from the evaluation and transformation of the electric potential at each electrode location in the Occam inversion. The inverted resistivity section and the calculated apparent resistivity pseudosection are updated until an acceptable RMS and L2-Norm are achieved or after eight iterations. In order to reduce the likelihood of mathematical artifacts, the number of iterations is controlled. Eight iterations is considered by convention to be the most iterations appropriate, keeping in mind that less iterations are preferred. The number of iterations, RMS, and L2-Norm are included in all inversions herein.

Chapter 3: Methodology

3.1 Equipment and Software

Electrical resistivity data were collected with the Advanced Geosciences Inc. (AGI) SuperSting Earth Resistivity IP & SP System. The SuperSting can take up to eight potential readings simultaneously per each current injection and is powered by two 12-V deep cycle marine batteries. In this study, 14 cables with four electrode connection points per cable (total of 56 electrodes) were used. The 56 stainless steel electrodes were 18 inches (46 cm) long and 0.87 inches (2.2 cm) in diameter (Figure 3.1a).

Arrays used in this study were chosen based on time of the test and vertical resolution of data. All tests were performed on active construction sites, and limiting the total time required for testing was critical because construction typically was stopped during testing. Vertical resolution was essential to determine the interface between the native material and the base of the MSE wall. The Wenner array was originally investigated but not used further because the array provides limited vertical resolution and extended testing time (over 75 minutes). The dipole-dipole array was used during early stages of testing because the array provides lateral and vertical resolution in less time than other arrays (approximately 1 hour). Ultimately, the inverted Schlumberger array was used exclusively because the array provided optimum vertical resolution in 30 minutes.

Stainless steel electrode stakes were hammered in the ground at desired equal distance spacing. The stakes were driven into the ground as deep as possible, thereby increasing contact between the stake and ground in order to minimize contact resistance. The cables were attached to the stainless steel electrode stakes by a spring attachment. The SuperSting was attached at the middle of the testing line; Figure 3.1b shows a typical field setup. While 3D tests are possible, they take 3 to 4 hours and do not provide the data quality and depth of investigation required for this study. It was determined that the most efficient method for testing MSE walls was to test the entire height of the wall and reach a depth in which the native material below the foundation of the wall was imaged.

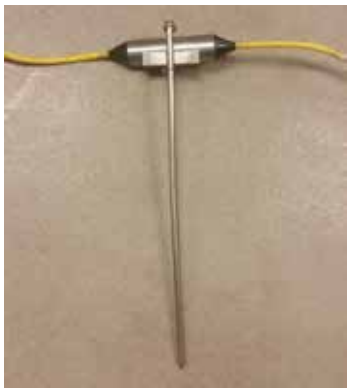

(a)

(b)

Figure 3.1: Equipment (a) Stainless Steel Electrode Setup; (b) Equipment Setup in the Field

After completing the setup, the contact resistance test was performed to verify that the cables were connected and the electrodes connected to the electrode stakes. An error code such as HVOVL typically indicates poor contact between the electrode and the ground. An INOVL error indicates a loose or improper connection. An issue with testing coarse aggregates is the difficulty obtaining proper contact between the electrode stake and the aggregates. The coarse angular aggregates do not contact the electrode stake as well as the fine-grained soil. Figure 3.2 shows the correlation of injected current and contact resistance. A lower contact resistance leads to an increased amount of current injected into the ground. The stronger the current signal, the more accurate the measurement.

The contact resistance test performed prior to ERI was vital in this study. A contact resistance between 0 and 20,000 Ohm provided adequate results with little noise (RMS values below 10%), data becomes uncertain and noisy between 20,000 to 40,000 Ohm (RMS around 10% typically), and more than 40,000 Ohm results in unusable data of poor quality (RMS greater than 10% typically). The larger the contact resistance, the lower the amount of injected current and the more inaccurate and noisy the measurement and vice versa. It was determined if results of the contact resistance test were high (greater than 40,000 Ohm) the entire ERI survey should be moved to an area that has recently been compacted as these regions provided better contact between the aggregate and the electrode stakes.

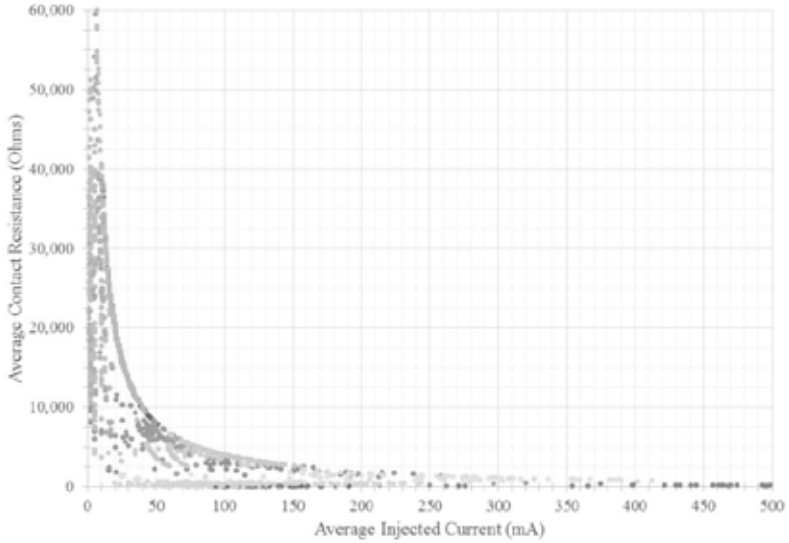

Figure 3.2: Correlation of Average Injected Current and Average Contact Resistance

3.2 Preliminary Electrical Resistivity Imaging Data

Six walls were designated by KDOT for testing: five MSE walls and one gravity retaining wall. Four of the five tested MSE walls contained geosynthetic reinforcement and one wall contained metal reinforcement. Each wall was tested during construction to determine optimal testing procedures for this study. The preliminary results were also used to determine the variation in ERI results during construction.

3.2.1 Geosynthetic Wall 1: Interchange of US Route 73 and Interstate 70

Geosynthetic Wall 1 (GW1) is an MSE wall at the interchange of US Route 73 (US-73) and Interstate 70 (I-70). The geogrid reinforced MSE wall is 1,160 ft (353.6 m) long and 5- 36 ft (1.5- 11.0 m) tall. Light weight compaction equipment was used from the face of the wall to up to 10 ft (3.0 m) from the face. Heavier compaction equipment and truck traffic were allowed 10 ft (3.0 m) and further from the face of the wall. Two preliminary test field setups are shown in Figure 3.3.

(a) (b)

Figure 3.3: GW1 Experimental Setup (a) June 18, 2014; (b) July 9, 2014

The characteristics of the test inversion details are shown in Table 3.1. Figure 3.4 shows the ERI image for profile GW1 614. The small boxes on the ground surface at the electrodes are spaced every 3 ft (0.91 m). The length of the profile is 162 ft (49.4 m) with 33.5 ft (10.2 m) penetration depth. The survey profile penetrated beyond the approximate wall height, shown as the dashed line, at the time of testing though there not does appear to be a resistivity anomaly corresponding to the leveling pad of the structure.

Table 3.1: Characteristics of GW1 614

Attribute	Value
Wall Height	30 ft (9.1 m)
Distance from Wall's Face	30 ft (9.1 m)
Electrode Spacing	3 ft (0.91 m)
Array	Dipole-dipole
Number of Iterations	6
Estimated Noise	5.0%
RMS	4.94%
L2	0.98

The profile GW1 614 in Figure 3.4 shows a body of high electrical resistivity (>200,000 Wcm) near the surface. This zone represents the poor contact between the electrodes and the aggregate and is not considered representative of the aggregate. The remaining resistivity values

from approximately 0.5 m to the base of the wall are between 12,000 and 100,000 Wcm. Low electrical resistivity regions less than 20,000 Wcm, represented by pale blue in Figure 3.4, are likely regions of increased compaction or where finer material is present. High electrical resistivity regions between 80,000 and 100,000 Wcm (yellow) are interpreted as regions where the compaction was not as thorough. The test was unable to image native material below the wall at approximately 30 ft (9.1 m) depth.

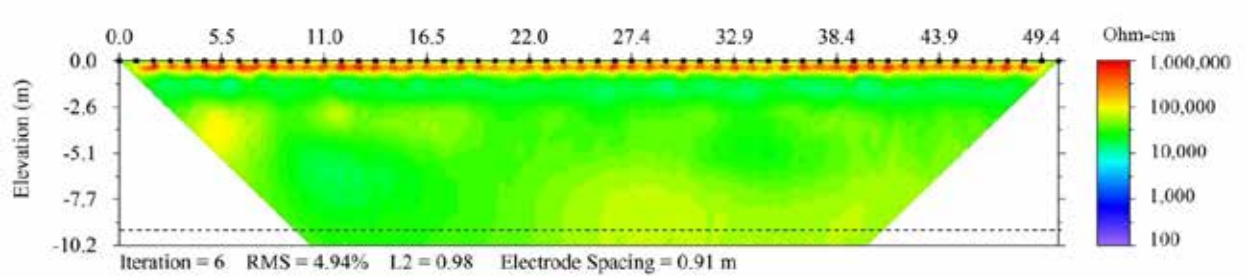

Figure 3.4: GW1 614 Inverted Resistivity Profile

An additional preliminary test was moved to a different section of the wall due to active construction at the previous testing location. The height of the wall varied approximately 15- 20 ft (4.5- 6.0 m), but no surface elevation change was present. This test was conducted near the interface where light-compaction and heavy-compaction equipment were used. The inverse Schlumberger array was used instead of the dipole-dipole array in order to increase vertical resolution and speed of data collection. Attributes of GW1 714 are given in Table 3.2

Table 3.2: Characteristics of GW1 714

Attribute	Value
Wall Height	15- 17 ft (4.5- 6.0 m)
Distance from Wall's Face	10 ft (3.1 m)
Electrode Spacing	2 ft (0.6 m)
Array	Inverse Schlumberger
Number of Iterations	4
Estimated Noise	5.0%
RMS	3.23%
L2	0.42

Figure 3.5 shows a body of resistivity similar to GW1 614, with high resistivity values near the surface and the remaining aggregate resistivity values between 20,000 and 80,000 W cm. Unlike GW1 614, the full height of the wall was imaged and native material below the wall can be seen where values decreased to below 10,000 Ohm-cm.

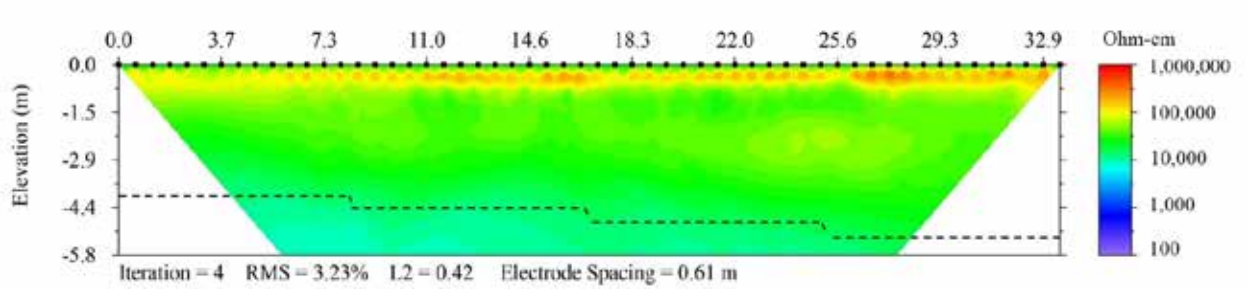

Figure 3.5: GW1 714 Inverted Resistivity Profile

3.2.2 Geosynthetic Wall 2: Overpass of 118th Street and Interstate 70

Geosynthetic Wall 2 (GW2) was located approximately 2 miles (3 km) east of Geosynthetic Wall 1 at the intersection of 118th Street and I-70. Because Geosynthetic Wall 1 and Geosynthetic Wall 2 were in close proximity to each other and were under construction at the same time, the aggregate source is the same. The geogrid reinforced wall shown in Figure 3.6 was 250 ft (76.2 m) long and 6.5- 23 ft (2.0- 7.0 m) tall. The test characteristics are given in Table 3.3.

Figure 3.6: GW2 Experimental Setup

Table 3.3: Characteristics of GW2 614

Attribute	Value
Wall Height	11.8- 16.4 ft (3.6- 5.0 m)
Distance from Wall's Face	2 ft (0.6 m)
Electrode Spacing	1 ft (0.3 m)
Array	Dipole-dipole
Number of Iterations	4
Estimated Noise	3.0%
RMS	2.99%
L2	0.99

The preliminary test was performed with 1-ft (0.3-m) spacing. Electrode spacing was limited due to active construction on the structure. Though the aggregate source was the same as Geosynthetic Wall 1, the inverted profile was dominated by much higher electrical resistivity values than GW1 614 or GW1 714. GW2 614 was performed within 2 ft (0.6 m) of the face of the wall. Also, only light-compaction equipment was utilized at the site. The increased electrical resistivity values compared to Geosynthetic Wall 1 are likely due to the location of the test and lighter compaction equipment. The increase in electrical resistivity values as compared to Geosynthetic Wall 1 will be discussed further in Section 4.1. The electrical resistivity of GW2 614 was 50,000 to 200,000 Wcm. The shortest section of the wall at the time of testing was 11.5 ft (3.6 m) between the start of the line and 3.67 ft (1.1 m). The base of the wall/top of the leveling pad in that area are in a region that is only marginally sensitive to the electrical resistivity survey and therefore not shown on the inverted resistivity profile.

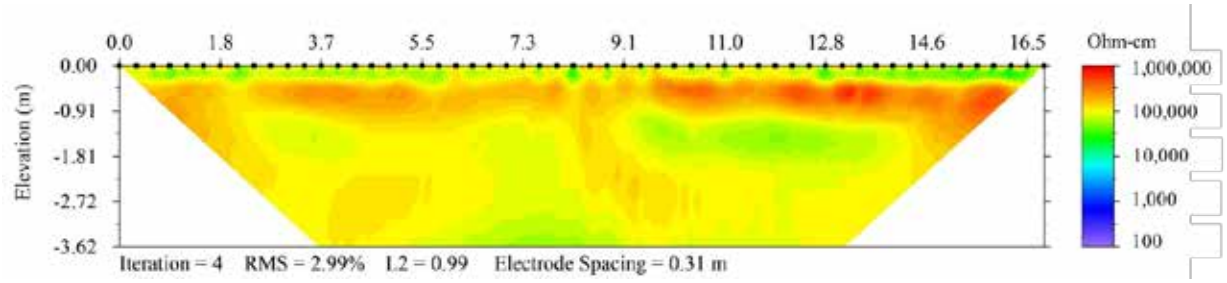

Figure 3.7: GW2 614 Inverted Resistivity Profile

3.2.3 Geosynthetic Wall 3: South Broadway Street and Centennial Drive

A sidewalk was added at the intersection of South Broadway Street and Centennial near a mall in Pittsburg, Kansas. A 387 ft (118 m) long MSE wall, Geosynthetic Wall 3 (GW3) shown in Figure 3.1, was added with a handrail to support a sidewalk and road without disturbing the mall's parking lot. Only light-compaction equipment was used at the site. The characteristics of GW3 714 are in Table 3.4. GW3 714 was performed during the final stages of wall construction, and only a small portion of the wall was tested due to active construction. Electrode stakes were placed into the ground surface with minimal effort compared to the previous testing sites, indicating that compaction at this site was minimal. Incomplete compaction at the surface was also apparent as the average contact resistance of the test was over 35,000 Ω. The high contact resistance led to ERI results that are not representative of the aggregate.

Table 3.4: Characteristics of GW3 714

Attribute	Value
Wall Height	6 ft (1.8 m)
Distance from Wall's Face	3 ft (0.9 m)
Electrode Spacing	1 ft (0.3 m)
Array	Inverted Schlumberger
Number of Iterations	8
Estimated Noise	5.0%
RMS	3.93%
L2	0.62

Figure 3.8 shows the inverted section of GW3 714 with extremely high electrical resistivity values of 1,000,000 Ωcm. The survey was able to image the native material below the foundation, but due to the poor quality data, the predicted electrical resistivity are likely not representative of the aggregate. No final test of Geosynthetic Wall 3 following compaction of the aggregate was possible due to the project schedule.

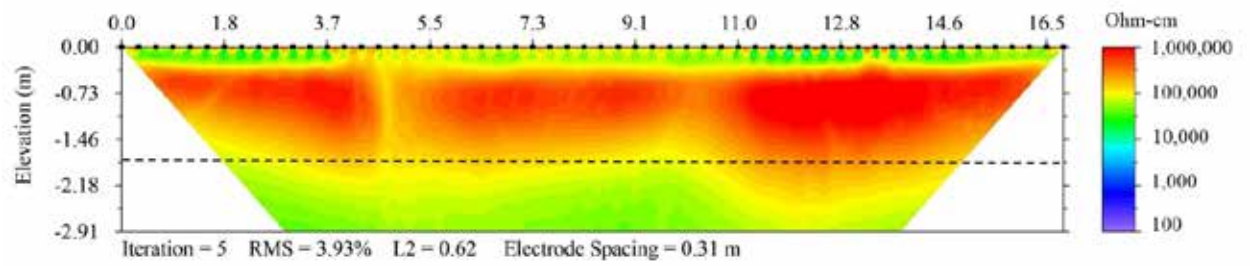

Figure 3.8: GW3 714 Inverted Resistivity Profile

3.2.4 Metal Wall 4: Interchange of Ridgeview and Kansas Highway 10

The overpass of Ridgeview above Kansas Highway 10 (K-10) was expanded in order to accommodate increased traffic flow, with abutments supported by MSE walls. These 4.5- 23 ft (1.4- 7.0 m) tall walls contained metal strip reinforcement approximately 0.25 inches (0.6 cm) thick and 2 inches (5 cm) wide that were anchored into the face of the wall. Reinforcement was placed at maximum horizontal spacing of 2.5 ft (0.75 m) and maximum vertical spacing of 1.5 ft (0.5 m). Each wall was 65 ft (20 m) long. Due to active construction during testing, only the northwestern MSE wall abutment was tested, shown in Figure 3.9. Light-compaction equipment was used from the face to 5 feet (1.5 m) from the face, and heavy-compaction equipment was used beyond 5 feet (1.5 m). MW4 914 was performed where heavy-compaction equipment was utilized.

Table 3.5 includes the characteristics of MW4 914.

Figure 3.9: MW4 Experimental Setup

Table 3.5: Characteristics of MW4 914

Attribute	Value
Wall Height	4.5- 23 ft (1.4- 7.0 m)
Distance from Wall's Face	10 ft (3.1 m)
Electrode Spacing	1 ft (0.3 m)
Array	Inverse Schlumberger
Number of Iterations	6
Estimated Noise	4.0%
RMS	3.82%
L2	0.92

Figure 3.10 depicts the electrical resistivity inverted section from profile MW4 1014. The approximate outline of the base and beginning of the wall are shown as the dashed line. Due to limited space, some of the experimental setup extended beyond the backfill of the wall and into native material. The electrical resistivity of MW4 914 is between 800 and 400,000 Wcm. The electrical resistivity values that are less than 5,000 Wcm (shown in blue) are likely due to the metallic reinforcement and migration of fine grained native material near the base of the wall. The influence of metallic reinforcement on the bulk electrical resistivity of the aggregate decreases within approximately 3.2 ft (1 m) of the surface. The profile shows a body of high resistivity (greater than 200,000 Wcm) between 41 and 49 ft (12.5 and 15 m). This zone likely represents an area of lower compaction or larger aggregate and was noted within several profiles, including the partially saturated study in Section 3.3.2 and the final profile on this structure in Section 4.3. The grain size distribution of a sample of material at MW4 was the only sample that classified as a well-graded gravel (GW) according to the Unified Soil Classification System (USCS). The wide range of particle sizes can be seen in Figure 3.9 as well. The impact of non-uniform backfill on in situ ERI testing is discussed further in Chapter 5. The overall electrical resistivity of the aggregate is similar to GW1 614 and GW1 714, between 15,000 and 80,000 W cm.

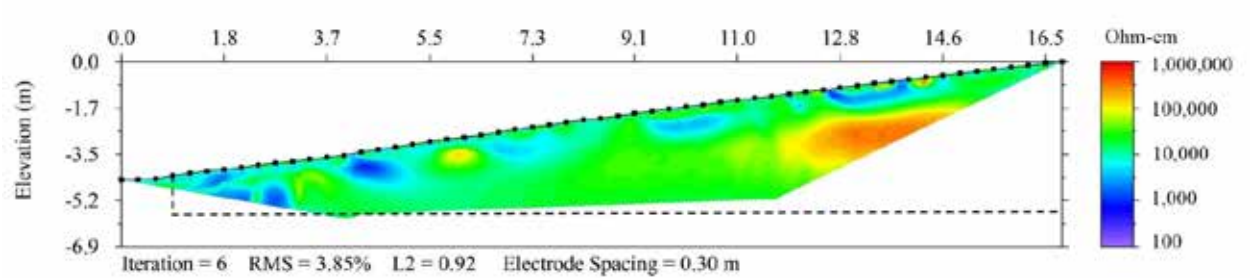

Figure 3.10: MW4 914 Inverted Resistivity Profile

3.2.5 Gravity Wall 5: Intersection of Haskell Avenue and East 31st Street

A gravity wall was built near the intersection of Haskell Ave. and East 31st St. in Lawrence, where the South Lawrence Traffic way was expanded. The 302 ft (92.1 m) long gravity retaining wall was added to retain a steep soil slope near one of the new roads. Figure 3.11 shows the experimental setup of a preliminary test at Gravity Retaining Wall 5 (GRW5).

Figure 3.11: GRW5 Experimental Setup

Table 3.6 includes the characteristics of the test. The preliminary test was run after a recent snow event. No snow was present at the time of testing, but the ground was frozen. Roller compaction was used except between 54 and 116 ft (16.5 and 35.5 m) where vibratory plate compaction was applied. The frozen aggregate increased the contact resistance at the surface leading to resistivity values over 1,000,000 Ω cm. These high surface resistivity are not considered representative of the aggregate.

Table 3.6: Characteristics of GRW5 215

Attribute	Value
Wall Height	6.5- 15 ft (2.0- 4.6 m)
Distance from Wall's Face	6 ft (1.8 m)
Electrode Spacing	3 ft (0.90 m)
Array	Inverse Schlumberger
Number of Iterations	6
Estimated Noise	10.0%
RMS	8.27%
L2	0.68

Despite the low quality of data due to the frozen ground, GRW5 215 imaged the foundation of the wall where it changed from aggregate (greater than 10,000 Wcm) to the native material (less than 10,000 Wcm).

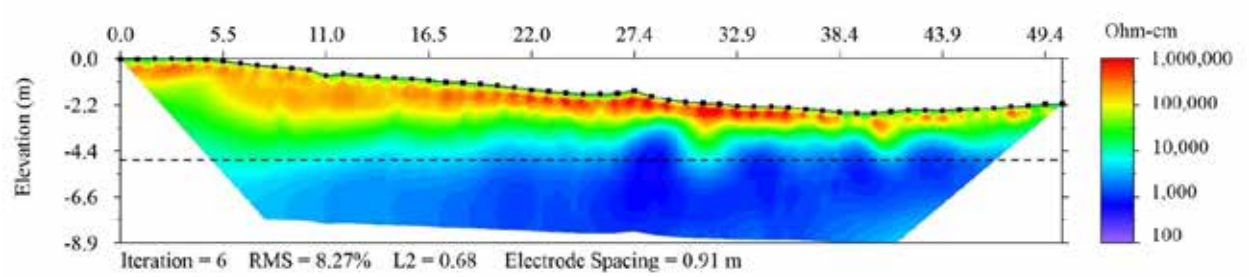

Figure 3.12: GRW5 215 Inverted Resistivity Profile

3.2.6 Geosynthetic Wall 6: Intersection of 31st St. and Louisiana St.

Similar to Gravity Wall 5, Geosynthetic Wall 6 (GW6) was built as part of the South Lawrence Traffic way expansion. The geogrid reinforced wall is 37 ft (11.31 m) long and 3 to 7.5 ft (0.91 to 2.29 m) tall with a minimum embedment of 3 feet (0.91 m) below the proposed ground. The characteristics of the preliminary test of GW4 615 are shown in Table 3.7. The preliminary data were gathered with a 1-foot (0.30-m) electrode spacing where the first 10 and last five electrodes extended beyond the reinforced backfill zone. The electrodes installed on the

structure averaged a contact resistance of 12,000 W, however the data were noisy. For this reason, the estimated noise was assumed to be 10.0% or twice the typical noise estimate and the resulting RMS in Figure 3.14 is 8.63%. A second test was possible which is included in Section 4.5.

Figure 3.13: GW6 Experimental Setup

Table 3.7: Characteristics of GW6 615

Attribute	Value
Wall Height	3- 7.5 ft (0.91- 2.29 m)
Distance from Wall's Face	1.5 ft (0.5 m)
Electrode Spacing	1 ft (0.30 m)
Array	Inverse Schlumberger
Number of Iterations	6
Estimated Noise	10.0%
RMS	8.63%
L2	0.74

Interestingly, the inverted section in Figure 3.14 does not image the full depth of the aggregate as shown on the retaining wall plans provided by KDOT, but rather stops at the existing ground line according to the plans. The resistivity of the aggregate that is imaged is similar to other structures, between 12,000 and 100,000 Wcm. The low resistivity (less than 1,000 Wcm) material surrounding the structure is soil. The final tests on this structure in Section 4.5 were able to measure the resistivity of the backfill down to the leveling pad of the structure, approximately 3 feet (1 m) below the proposed ground surface.

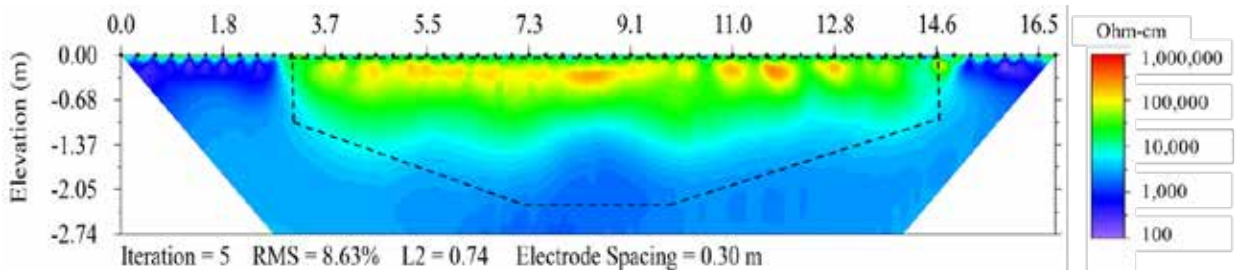

Figure 3.14: GW6 615 Inverted Resistivity Profile

3.3 Partially Saturated Electrical Resistivity Imaging Data

Three surveys were run one day after heavy rainfall. These were conducted to understand the influence of water on the predicted electrical resistivity of the aggregate and to determine if partially saturated experiments can be compared directly to AASHTO T 288.

3.3.1 Partially Saturated Geosynthetic Wall 2

A partially saturated survey was conducted on Geosynthetic Wall 2 approximately 1 year after the wall was complete. Geosynthetic Wall 2 was covered with grass (Figure 3.15) which allowed for better contact with the electrodes as compared to tests run on aggregate. The average contact resistance was 250 W. Attributes of Test SGW2 are outlined in Table 3.8.

Table 3.8: Characteristics of SGW2 515

Attribute	Value
Wall Height	10- 23 ft (3.0- 7.0 m)
Distance from Wall's Face	4 ft (1.2 m)
Electrode Spacing	3 ft (0.91 m)
Array	Inverted Schlumberger
Number of Iterations	4
Estimated noise	3
RMS	2.74%
L2	0.84

Figure 3.15: SGW2 Experimental Setup

The approximate foundation of the wall is shown in dashed lines on the inverted resistivity section. Unlike the previous survey, there is a continuous body of low resistivity of 3,000 to 5,000 Wcm across the upper surface to 4 ft (1.2 m). This lower resistivity is attributed to the saturated topsoil that resulted from the recent rains which also reduced the resistivity of the aggregate near the surface. The bulk electrical resistivity of the aggregate is 21,000 to 100,000 Wcm, lower than the previous surveys on this structure.

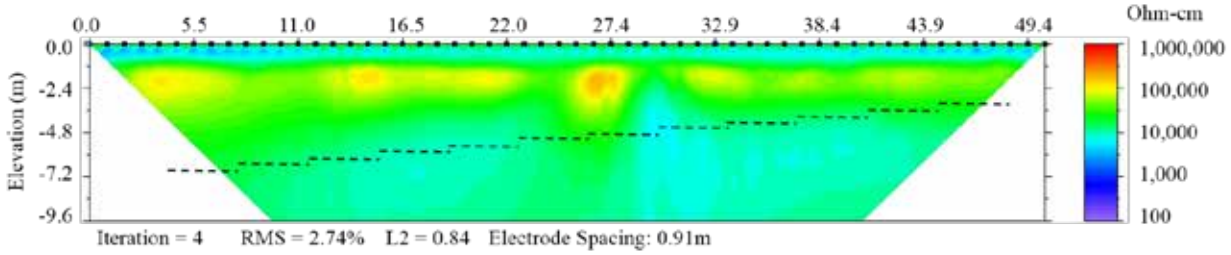

Figure 3.16: SGW2 515 Inverted Resistivity Profile

3.3.2 Partially Saturated Metal Wall 4

The metallic wall was also tested following days of heavy rain and approximately 1 hour after the rain stopped. Unlike other structures in this study, the backfill of Wall 4 was sand with 99.7% of the material retained on the No. 200 (2 *m*m).

Table 3.9 lists the characteristics of the survey. The saturated sand resulted in an average contact resistance of 1,300 W.

Table 3.9: Characteristics of SMW4 1014

Attribute	Value
Wall Height	4.6- 23 ft (1.4- 7.0 m)
Distance from Wall's Face	10 ft (3.1 m)
Electrode Spacing	1 ft (0.3 m)
Array	Inverted Schlumberger
Number of Iterations	4
Estimated Noise	5.0%
RMS	4.04%
L2	0.64

The resistivity profile of SMW4 1014, where water was present during testing, is shown in Figure 3.17. Note that the body of resistivity that is higher than the surrounding aggregate starting at approximately 12 m (39.4 ft) across the survey in Figure 3.10 is still present, though the resistivity is 40,000 to 60,000 Wcm instead of over 200,000 Wcm.

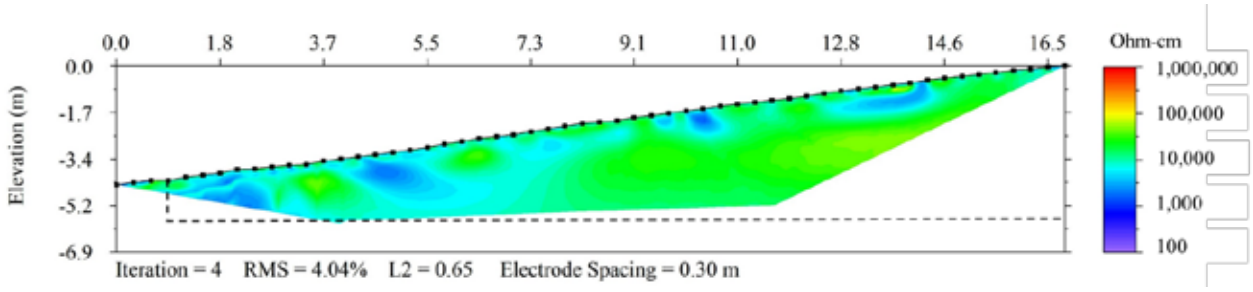

Figure 3.17: SMW4 1014 Inverted Resistivity Profile

Overall the electrical resistivity of the inverted section decreased due to the presence of water from previous rain events and rain during testing. The low resistivity zones near the surface are attributed to the metal reinforcement. The overall electrical resistivity has decreased due to the presence of water in the wall.

3.3.3 Partially Saturated Gravity Wall 5

The gravity wall was near completion during the saturated test, with approximately 1.5 ft (0.46 m) retained soil from the excavation placed over the aggregate with a filter fabric between the two materials. The retained material provided adequate contact between the electrode stakes

and the ground and was partially saturated due to heavy rains during previous weeks. The characteristics of SGR5 515 are shown in Table 3.10.

Table 3.10: Characteristics of SGR5 515

Attribute	Value
Wall Height	12- 23 ft (3.7- 7.0 m)
Distance from Wall's Face	6 ft (1.8 m)
Electrode Spacing	3 ft (0.91 m)
Array	Inverse Schlumberger
Number of Iterations	5
Estimated Noise	3.0%
RMS	2.81%
L2	0.87

Figure 3.18 imaged the native material at the ground surface (approximately 1,000 Ohm-cm), the aggregate backfill (6,000 to 30,000 Ohm-cm), and the native soil below the foundation (less than 500 Ohm-cm). As expected, the results showed a material with a lower electrical resistivity than previous testing; however, the preliminary survey of GRW5 was conducted when the ground was frozen. Note that the scale in Figure 3.18 has been changed to visualize the backfill.

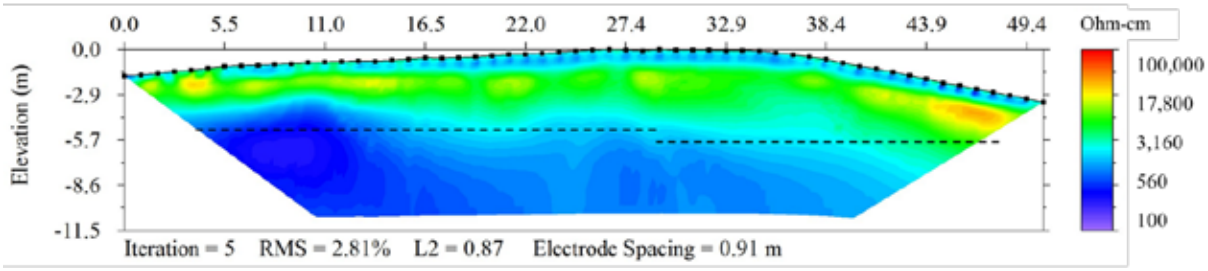

Figure 3.18: SGR5 515 Inverted Resistivity Profile

The partially saturated results were also lower than the final test discussed in Section 4.4. Lower values are attributed to the presence of water within the wall due to recent rain events. SGW2, SMW4, and SGR5 give insight to the in situ electrical resistivity when in the worst case scenario. All tests show that the presence of water greatly reduces the electrical resistivity, thus increasing the corrosion potential, though the bulk resistivity for all structures are still above the

T 288 classification of noncorrosive material. The higher resistivity measurements suggest that T 288 may in fact be over conservative for these materials.

ERI results from the six walls demonstrated that the field method can be applied to measure the electrical resistivity of retaining wall aggregate backfill. These results, however, were constantly higher than electrical resistivity results gathered in the laboratory using AASHTO Standard T 288-12 (2012). The preliminary surveys showed that geosynthetic reinforcement had no effect on the electrical resistivity results. Metal reinforcement altered electrical resistivity values near the surface, but the effect dissipated with depth. Water within the backfill materials was shown to lower electrical resistivity results. Due to the subjective nature of the qualitative interpretation of these surveys, a post-processing data algorithm was developed to determine the bulk electrical resistivity at each wall.

3.4 Quantitative Post-Processing Algorithm

A quantitative post-processing algorithm was used to determine average bulk resistivity of each in situ test, utilizing inverted data in order to reduce the qualitative interpretation of the ERI section. Only resistivity values representative of the wall were used in the bulk calculations; therefore, data below the wall's foundation, mathematical artifacts due to poor contact at the surface, and where surveys were extended off walls into native soils were removed. A histogram of the inverted resistivity data was created for each final electrical resistivity survey. As an example, Figure 3.19 is the histogram for GW1 614.

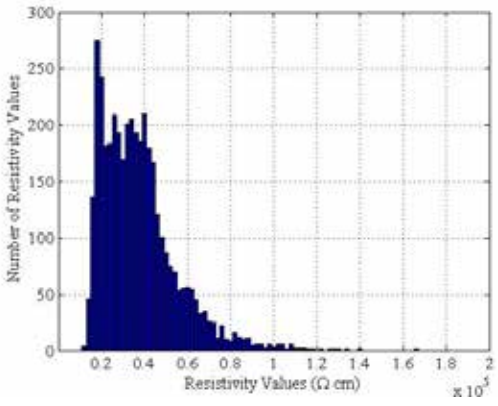

Figure 3.19: Histogram of GW1 614

Based on a goodness-of-fit test described by Baecher and Christian (2005), the data followed a lognormal distribution. This was determined by plotting the Cumulative Density Function (CDF) of the resistivity data and log of the data as a normal distribution. A linear fit indicated a good fit of the data to the distribution. The norm of the residuals was used to calculate the goodness of fit of the data to a linear approximation. The mean μ of each data set was found as:

$$\mu = \frac{\sum x_i}{n} \qquad \textbf{Equation 3.1}$$

Where:

The numerator is the sum of all observations x_i and the denominator is the total number of observations, n.

The standard deviation is:

$$\sigma = \sqrt{\frac{1}{n}\sum_{i=1}^{i=n}(x_i - \mu)^2} \qquad \textbf{Equation 3.2}$$

Where all terms have been defined.

The normal CDF is determined by:

$$F(x|\mu,\sigma) = \frac{1}{\sigma\sqrt{2\pi}}\int_{-\infty}^{x} e^{\frac{-(t-\mu)^2}{2\sigma^2}}\,dt \qquad \textbf{Equation 3.3}$$

In which:

t is each data value, and

x is the interval of data.

The result is the probability that an observation will lie in the given interval from a normal distribution. In order to determine the lognormal CDF, the mean μ and standard deviation σ of the log data were calculated. The lognormal distribution has a mean m:

$$m = \log\left(\mu^2 \Big/ \sqrt{v+\mu^2}\right) \qquad \textbf{Equation 3.4}$$

And variance *v*:

$$s = \sqrt{\log\left(v/m^2 + 1\right)} \qquad \textbf{Equation 3.5}$$

Where:

m and s are the mean and standard deviation of the log of the data, respectively.

The lognormal CDF is defined as:

$$F(x|m,s) = \frac{1}{s\sqrt{2p}} \int_0^x \frac{e^{\frac{-(\ln(t)-m)^2}{2s^2}}}{t} dt \qquad \textbf{Equation 3.6}$$

As mentioned, the norm of the residuals was used to estimate the goodness of fit of the linear fit of the data. Norm of residuals is defined as:

$$norm = \sqrt{\sum_{i=1}^{n} d_i^2} \qquad \textbf{Equation 3.7}$$

Where:

d_i is the difference between the ith predicted data and the measured data.

A perfect linear fit of the data would produce a norm of residual of zero. Table 3.11 contains the norm of residuals from the normal distribution of the data and the log of the data plotted in CDFs. The lognormal norm of residuals is less than the normal norm of residuals for each test, implying that the data follow a lognormal distribution. The lognormal distribution was also used because each test was independent and the results cannot be negative.

Table 3.11: Norm of Residuals from the Normal Distribution of Normal and Lognormal CDFs

Test		**1**	**2**	**3**	**4**	**5**	**6**	**7**	**8**	**10**
Norm of Residuals	**Normal**	4.8	3.5	2.3	5.3	4.6	5.9	3.6	4.6	5.3
	Lognormal	2.6	2.7	2.1	3.3	3.9	4.7	2.9	2.2	3.8
Test		**11**	**12**	**13**	**14**	**15**	**16**	**17**	**18**	**19**
Norm of Residuals	**Normal**	6.0	9.4	7.6	9.0	5.4	5.1	5.9	3.0	4.5
	Lognormal	4.0	3.6	4.7	4.5	3.4	2.2	3.7	2.4	3.1

After determining that the data were lognormally distributed, the lognormal Probability Density Function (PDF) of the data was used to determine bulk resistivity of each survey. Geosynthetic Wall 3 was excluded from the processing due to the poor quality of the data (Section 3.2.3). The lognormal PDF is:

$$f\left(x|m,s\right)=\frac{1}{xs\sqrt{2p}}e^{\frac{-(\ln x-m)^2}{2s^2}}$$

Equation 3.8

In which the variables have been previously defined.

The PDF (Figure 3.20) was used to visualize the distribution of the data. An advantage of the PDF is that the PDF of all tests on the same wall can be plotted as one, rather than comparing histograms side by side. The peak of the PDF may be greater than 1, because the PDF is the probability density, or the probability per unit value of electrical resistivity. The integral of the density function may not exceed 1. The peak of the PDF is 50% of the data (50% of the data lies to the left or right of the peak).

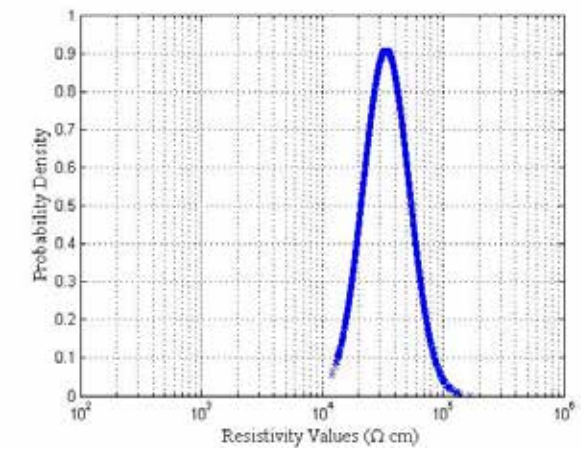

Figure 3.20: PDF of GW1 614

The 95% confidence interval of the mean bulk electrical resistivity of each test in the lognormal probability distribution was calculated in order to describe the mean of the data for each wall. A confidence interval of 95% implies that 95% of sampling would provide an interval

that includes the mean (m), and only 5% of sampling would provide an inaccurate interval (Devore, 2004). In other words, a confidence interval of 95% means that 95% of any sample taken from that particular ERI test will produce a mean within the calculated confidence interval. The large-sample confidence interval for the population mean for any population distribution is represented in the following equation:

$$\bar{x} \pm z_{a/2} \frac{s}{\sqrt{n}}$$

Equation 3.9

In which:

$\bar{x}$ is the samples mean,

$z_{a/2}$ is the critical value,

s is the sample standard deviation, and

n is the number of observations.

The critical value is a set constant based on the desired confidence, 1.96 for a 95% confidence interval. A confidence interval with a small range suggests that more is known about the mean; a wide range suggests a larger range of variability of the mean. In other words, a small range implies more uniform ERI results, while a wide range implies a less uniform distribution of electrical resistivity results. Some variability was expected within the backfill due to varying degrees of compaction, migration of finer material, and the inherent non-uniqueness of inverted resistivity. The confidence interval captures some of the variability while providing the mean of the material.

Chapter 4: Electrical Resistivity Results

Many of the initial surveys for this study were used to determine optimal testing protocol for this application, such as the array, electrode spacing, and testing time. Because the degree of compaction affects the bulk resistivity, the tests in this chapter are the final surveys of five of the six walls. Unfortunately, one site was not successful because the aggregate was not compacted at the surface during testing, which caused poor contact between the electrodes and the aggregate. Also, the project schedule did not allow a retest once the aggregate was compact.

4.1 Geosynthetic Wall 1

The final test was performed on August 12, 2014. A sample of the aggregate was found to have an electrical resistivity of 3,808 Ωcm per T 288 (moderately corrosive). The testing location was in the same area as GW1 614. The test was again at the interface of light and heavy compaction equipment and truck traffic was prohibited. The section of the wall shown in Figure 4.1 was at maximum height of 36 ft (11 m), but the depth of investigation did not penetrate to the foundation of the wall.

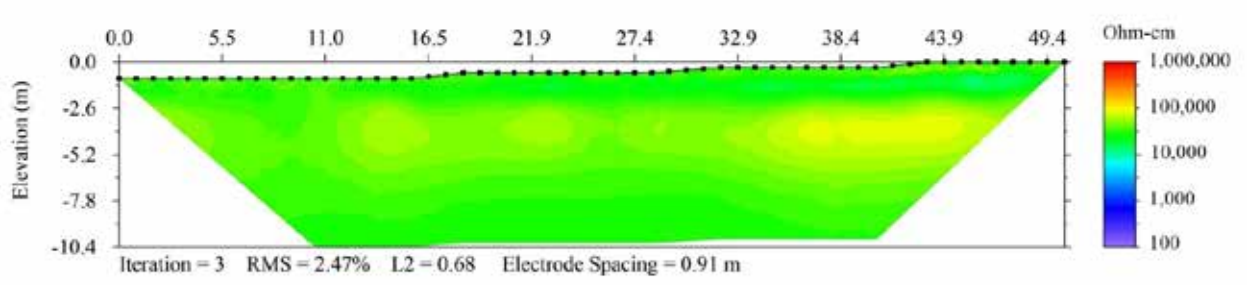

Figure 4.1: GW1 Final Inverted Resistivity Section

The band of high resistivity (approximately 50,000-80,000 Ωcm) across the inversion in Figure 4.1 was likely a result of a layer of aggregate that was not compacted as thoroughly as the layers above and below. Data utilized for post-processing were from the inverted section only. The post-processing histogram shown in Figure 4.2a demonstrates variability in the backfill more clearly, and the confidence interval of the lognormal probability distribution gives a range

of the expected mean of the backfill. Figure 4.2b shows the variability of the data on the same scale as Figure 4.1, between 100 and 1,000,000 Wcm.

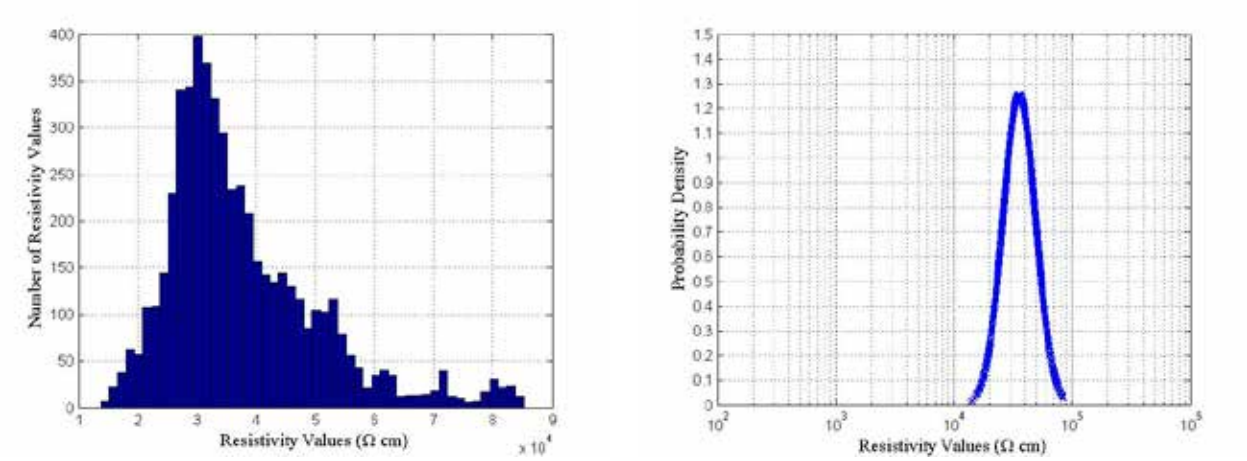

(a) (b)

Figure 4.2: GW1 Final (a) Histogram; (b) PDF

The bulk resistivity confidence interval of the aggregate was 37,078- 37,967 Wcm. The minimum and maximum resistivities of the backfill were 13,716 Wcm and 85,166 Wcm, respectively. As expected, electrical resistivity values were approximately one order of magnitude greater than T 288 results because the AASHTO standard was performed on fine, saturated material.

4.2 Geosynthetic Wall 2

GW1 and GW2 were in close proximity to each other and were under construction at the same time so the aggregate source was the same. The same aggregate was expected to have approximately the same bulk resistivity as GW1. The ERI survey in Figure 4.3 was run when the wall was almost complete and varied in height from 10 to 22 ft (3 to 6.7 m). Although the surface of the survey was flat, the bearing foundation was not flat. The stair step of the base of the wall/top of the leveling pad foundation for Geosynthetic Wall 2 is shown in Figure 4.3 with dashed lines. The survey was not conducted over the tallest part of the wall.

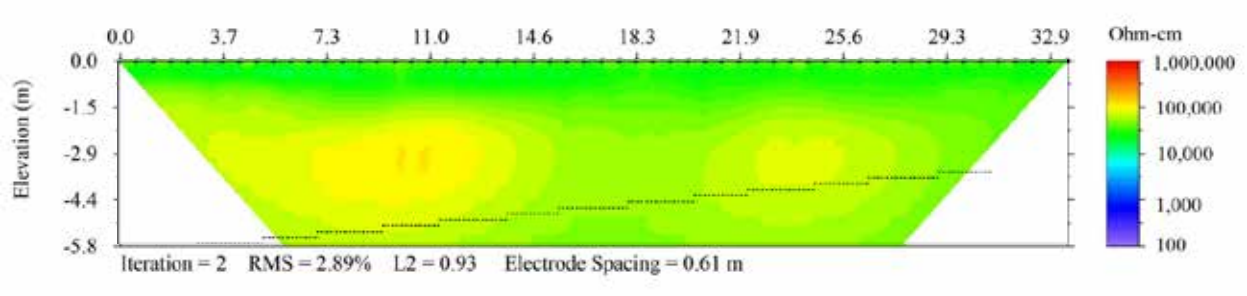

Figure 4.3: GW2 Final Inverted Resistivity Section

A comparison of Figure 4.1 and Figure 4.3 shows that the bulk resistivity of GW2 was higher than GW1 even though the aggregate source was identical. The region of increased resistivity between 12 and 48 ft (3.7 and 14.6 m) is discussed in Section 4.1. Resistivity was also higher between 71.9 and 84 ft (21.9 and 25.6 m), possibly due to the proximity of the leveling foundation. These regions of high resistivity make the distribution in Figure 4.4a appear to be approximately bimodal.

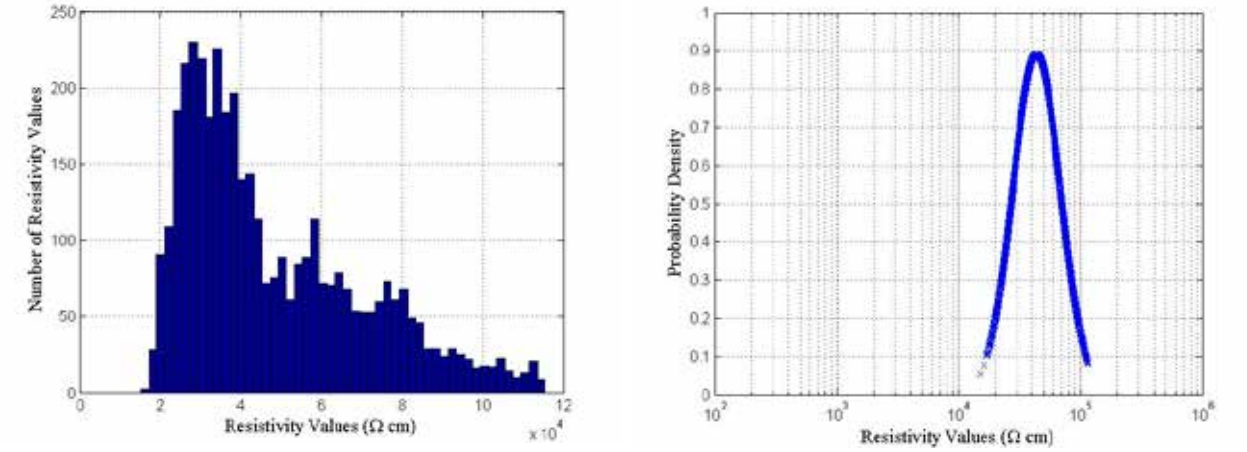

(a) (b)

Figure 4.4: GW2 Final (a) Histogram; (b) PDF

The bulk resistivity of Wall 2 was 47,162- 48,926 Wcm at the 95% confidence interval and the minimum and maximum resistivities were 15,047 and 115,580 Wcm, respectively. Although only 27% of the data were over 60,000 Wcm, the confidence interval increased by approximately 10,000 Wm compared to the same aggregate of GW1. The difference of

approximately 10,000 Wcm was likely due to variation in compaction between the walls. GW1 was over 13.1 ft (4 m) taller than GW2; therefore, the length of reinforcement required to support the wall and the depth of backfill behind the wall were also significantly larger. This allowed heavier compaction equipment to be utilized on GW1, thereby reducing the void space in the aggregate and the bulk electrical resistivity.

Figure 4.5 shows results of Figure 4.3 along with the first survey of GW2. Figure 4.5b was conducted three weeks before Figure 4.5a. Both surveys were conducted 2 ft (0.61 m) from the face of the wall. As shown in the figure, the bulk resistivity of GW2 at its preliminary stage was much higher than bulk resistivity at the final stage, potentially due to poor compaction of the aggregate. Interestingly, the resistivity decreased over time, implying that, after multiple passes of compaction equipment, compaction improved, but not enough to generate resistivity similar to GW1.

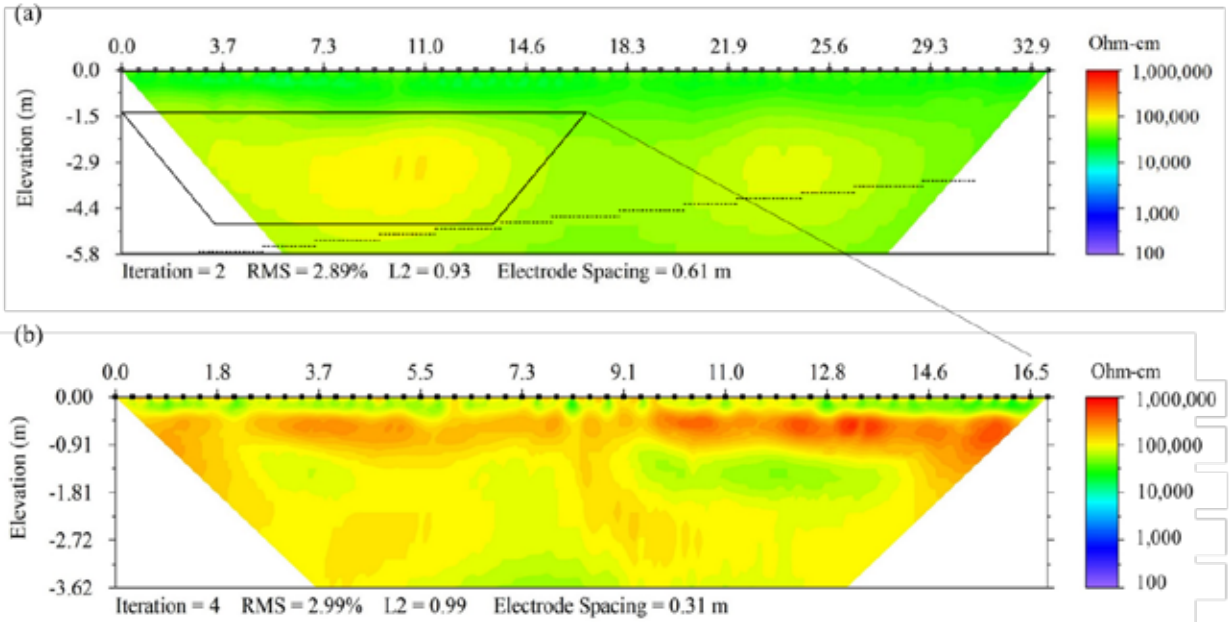

Figure 4.5: GW2 (a) GW2 Final Inverted Resistivity Section; (b) GW2 614

Figure 4.5a yields the expected bulk resistivity for this aggregate in the top 4.9 ft (1.5 m), demonstrating that GW2 could also utilize resistivity for quality control of aggregate compaction. Unlike soil compaction, in situ CQA tests are not utilized to verify uniform compaction and to a desired density on MSE structures. Typically, CQA is ensured by specifying

the maximum thickness of each aggregate layer and the number of equipment passes over the layer. Figure 4.5 also reveals a limited depth to which compaction equipment at the surface can improve compaction in lower layers.

4.3 Metal Wall 4

Compared to the polymeric geogrid used in GW1 and GW2, the risk of reinforcement corrosion in MW4 required that the aggregate source have a higher resistivity according to T 288. The T 288 measurement for MW4 was 6,036 Wcm (mildly corrosive). Figure 4.6 shows zones of expected high resistivity between 0 and 42 ft (12.8 m) based on T 288, with intermittent zones between electrodes of lower resistivity. Conductivity regions (less than 10,000 Wcm) between 0 and 42 ft (12.8 m) were likely due to metallic reinforcement that influences bulk resistivity of the aggregate. The effects of metallic reinforcement decreased at depths greater than approximately 4.9 ft (1.5 m) below the surface, but the aggregate was still notably lower across the inversion in several locations. When comparing Figure 4.6 to other final inverted sections, the majority of the backfill appears similar to other structures (approximately 10,000 W cm, shown in green) despite the higher T 288 test sample.

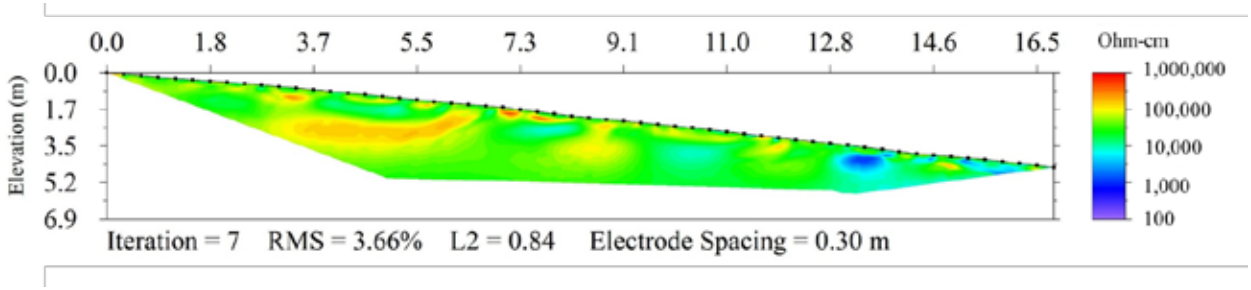

Figure 4.6: MW4 Final Inverted Resistivity Section

When post-processing the metallic wall, only data shown between 0 and 12.8 m were included. Due to limited space at this wall caused by construction activities, the survey line extended into native material at the base of the wall which included a large amount of highly conductive fine-grained material. Figure 4.7a shows that more data points were significantly higher (over 100,000 Wcm) than GW1 and GW2. This was expected because of the increased likelihood of corrosion of the metallic reinforcement as compared to the polymeric

reinforcement. In addition, lower resistivity (less than 10,000 Wcm) values due to metallic reinforcement were observed for MW4 as compared to the other walls.

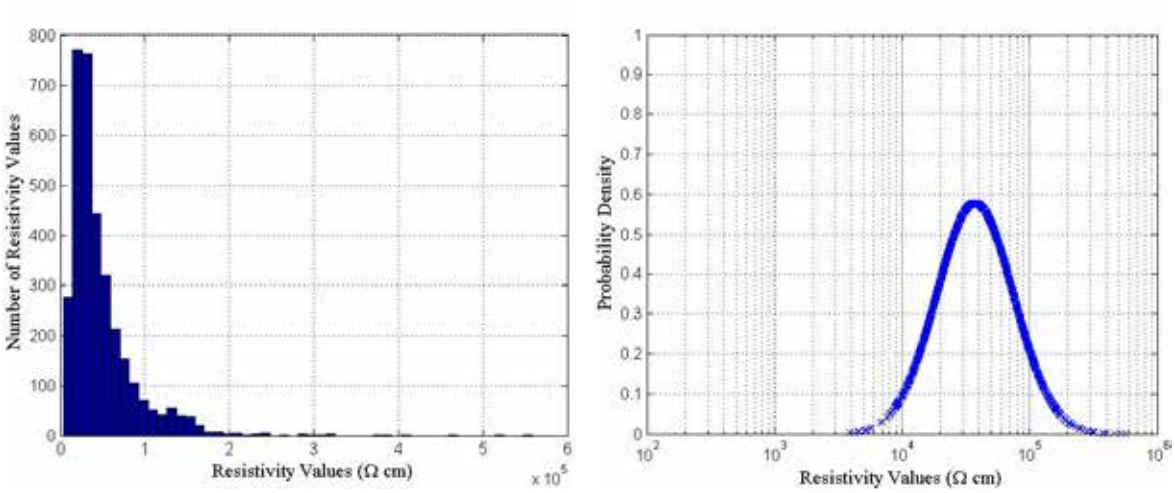

(a) (b)

Figure 4.7: MW4 Final (a) Histogram; (b) PDF

The minimum resistivity of MW4 was 3,848 Wcm; however, this occurred at the surface of the backfill and is likely due to the metallic reinforcement. Additional testing of MSE walls containing metal reinforcement is needed in order to further define the effect of metal reinforcement on ERI. The 95% confidence interval of the mean bulk resistivity of MW4 was 45,719- 48,988 Wcm, similar to GW2. The maximum resistivity of the backfill was 558,916 W cm.

4.4 Gravity Wall 5

The initial test of the gravity wall (GRW5 215) was conducted while the ground was frozen, leading to an over estimation of the electrical resistivity near the surface. The final test was run when the wall was 21 ft (6.4 m) at its tallest point. The wall was compacted using heavy equipment, except in a region where the wall was not wide enough to allow passage for a roller. The plans note that there was Stranger formation across the site and local lithologic logs note that there was clay over weather shale to limestone. The profile shown in Figure 4.8 was run from the beginning of the wall where the backfill was 2 ft (0.6 m) deep to 10 ft (3 m). The top of the

foundation is shown with the black dashed line. Beneath the foundation is likely a clay layer with a shale outcrop in the middle. The low resistivity beneath the foundation (less than 100 Wcm) influences the bulk response above the foundation where measured resistivity is low.

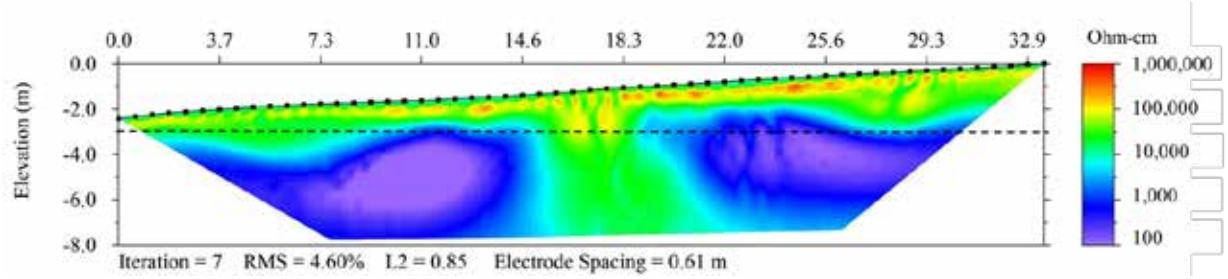

Figure 4.8: GRW5 415 Final Inverted Resistivity Section

The histogram of the aggregate data above the top of the foundation and the corresponding PDF are shown in Figure 4.9. Due to the low resistivity data above the foundation, the PDF in Figure 4.9b shows much more spread in the data than previous structures. The minimum resistivity of this backfill was 166 Wcm and the maximum was 559,878 Wcm.

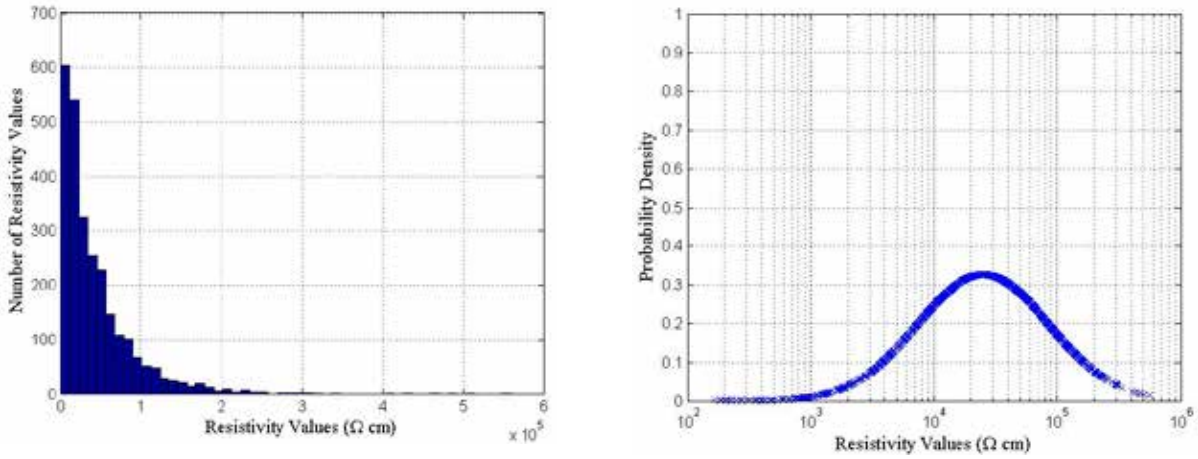

(a) (b)

Figure 4.9: GRW5 Final (a) Histogram; (b) PDF

The T 288-12 results showed that the aggregate had an electrical resistivity of 3,895 Wcm (moderately corrosive). The low resistivity layer beneath the foundation was imaged

in all surveys of GRW5 though it was the most pronounced in the final inversion. Because they are lowest in the final inversion, they are likely water that was beneath the structure at the time of testing. The 95% confidence interval of the aggregate was 48,388- 57,539 Wcm.

4.5 Geosynthetic Wall 6

The preliminary survey of GW6 in Section 3.2.6 was not able to image the full depth of the aggregate. A second survey was conducted with smaller electrode spacing to reduce the influence of the native material at the beginning and end of the survey. The backfill was not fully compacted at the time of testing, leading to higher resistivity values in the upper 2 feet (0.6 m).

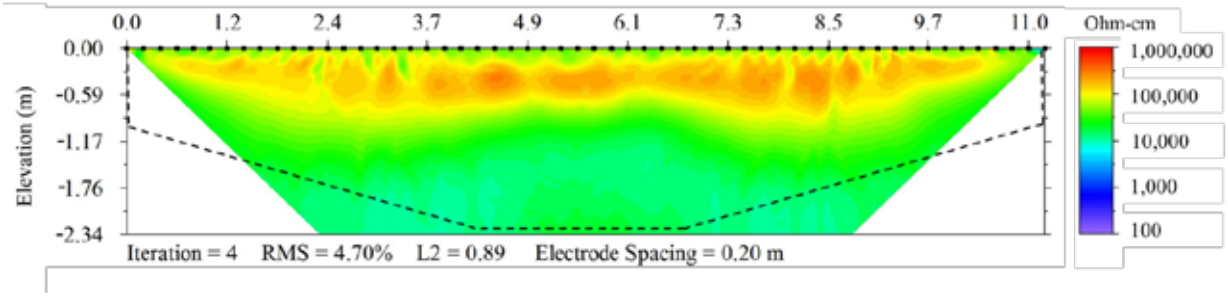

Figure 4.10: GW6 Final Inverted Resistivity Section

The body of low electrical resistivity in Figure 3.14 was no longer measured during the final test and was likely water at the base of the structure in the preliminary survey. Despite the high surface resistivity values, the bulk of the aggregate is similar to the other structures. Post processing of Figure 4.10 assumed that the structure was built with the 0.91 m depth of embedment shown on the plans. As shown in Figure 4.11, the range of electrical resistivity values for this structure was much wider than the first four walls; this will be discussed further in Chapter 5. The high resistivity values near the surface increase the confidence interval to be much higher than previous structures. The 95% confidence interval for GW6 was 65,203- 69,629 Wcm. The maximum resistivity of GW6 was 359,840 Wcm and the minimum was 2,829 Wcm. The maximum resistivity was due to poor electrode contact leading to higher resistivity values near the surface.

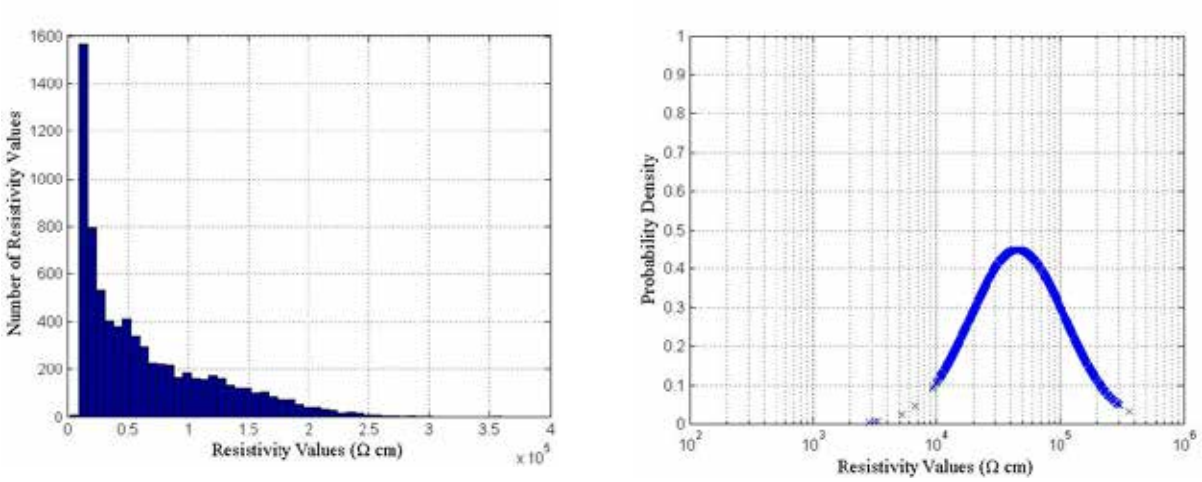

(a) (b)

Figure 4.11: GW6 Final (a) Histogram; (b) PDF

Chapter 5: Conclusions

This report presents an experimental study that assessed the feasibility of utilizing ERI surveys to determine average bulk electrical resistivity of backfills for earth retaining structures. ERI surveys of aggregate backfill provide data on the uniformity of the bulk electrical resistivity during and after construction, corrosion potential, and potentially construction quality assurance information. A quantitative post-processing algorithm was developed in this research to remove the qualitative uncertainty of ERI results and to provide a bulk electrical resistivity range for each wall (Table 5.1). As expected, these results are significantly higher than those gathered through laboratory experimentation because the materials and test conditions are different. AASHTO Standard T 288-12 (2012) laboratory test requires that the test sample pass a No. 10 sieve (2.0 mm) and a minimum resistivity measurement be recorded, which is achieved when the material is in a slurry or water-dominated state. These results are likely not indicative of the in-place backfill conditions as the backfill should never be fully saturated when proper construction is achieved and water can drain through and away from the retaining walls. Three of the six walls were tested 24 hours after a rain event to measure the as-constructed minimum resistivity. In order to directly compare ERI to T 288 or other laboratory measurements, the degree of saturation between the sample and field must be similar.

Table 5.1: Summary of Bulk Electrical Resistivity Testing Results

Wall	AASHTO T 288-12 (Ωcm)	ERI 95% Confidence Interval (Ωcm)	Mean ERI (Ωcm)
Geosynthetic Wall 1	3,808	37,150 – 37,935	37,605
Geosynthetic Wall 2		47,162 – 48,926	48,106
Partially Saturated Geosynthetic Wall 2		28,282 – 30,899	29,249
Geosynthetic Wall 3	Not provided	N/A	N/A
Metal Wall 4	6,036	45,719 – 48,988	47,924
Partially Saturated Metal Wall 4		12,743 – 13,502	13,087
Gravity Wall 5	3,895	48,388 – 57,539	44,750
Partially Saturated Gravity Wall 5		4,533 – 4,919	4,768
Geosynthetic Wall 6	Not provided	65,203 – 69, 629	65,883

ERI can produce electrical resistivity distributions of aggregate backfill of MSE walls and retaining walls. The advantage of using ERI is that it provides data of the entire wall or a section of the wall rather than a point source obtained in the laboratory, yielding more information on the backfill. Final ERI surveys were applied to four MSE walls and one gravity wall. The post processing summary of the five walls is shown in Figure 5.1. The post processing PDF shows the variability of the resistivity, where more narrow PDFs indicate more uniform bulk electrical resistivity measurements. The distribution of electrical resistivity of aggregate backfill is a function of the particle size distribution, the degree of compaction, and degree of saturation. In a complementary laboratory study by Brady, Parsons, and Han (2016), samples were collected from five of the walls tested in this study. In Figure 5.2, Gray I-70/K-7 was sampled from GW1 compacted backfill, Colored I-70/K-7 was sampled from the stockpile used for GW1 and GW2, Ridgeview was MW4, SLT was GRW5, Pittsburg was GW3 not included in the final surveys, and GW6 was not collected but is likely the same material as SLT. GW1 was the most uniform ERI survey and PDF. GW1 was compacted with a heavy roller and was subject to truck traffic. Additionally GW1 samples had the most uniform grain size distributions in Figure 5.2. These samples both classified as poorly graded gravels (GP) according to the Unified Soil Classification System. The maximum size of the gravel for both samples was 1 inch (25 mm).

Although GW2 utilized aggregate from the same quarry, only a vibratory plate compactor weighing less than 1,000 pounds (454 kg) was used in the test area. This led to a higher bulk electrical resistivity confidence interval and wider range in the data shown in Figure 5.1. MW4 yielded a wider spread in resistivity data in Figure 5.1 than GW1 and GW2. Unlike the other structures, MW4 contained Metal SINE-Strip reinforcement and the metal may have influenced the resistivity measurements near the reinforcement at the surface. A region of high resistivity was noted in all tests at MW4 which was likely large diameter gravel. According to the sample collected by Brady et al. (2016), the Ridgeview sample was a well graded gravel (GW) with a maximum aggregate size of 3 inches (75 mm). Large diameter aggregates can also be seen in Figure 3.9. This wide range of particle sizes is reflected in the increased confidence interval for the sample.

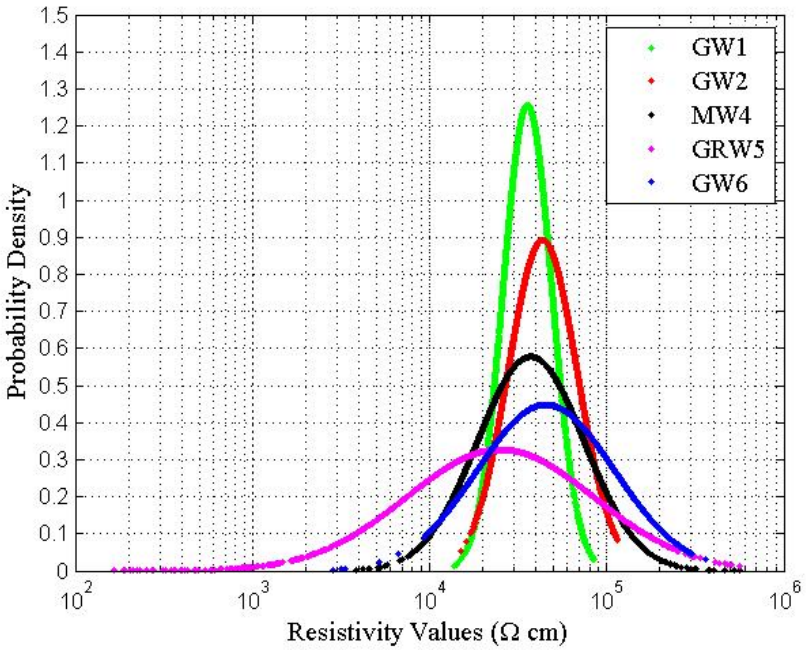

Figure 5.1: Summary of Measured Bulk Resistivity

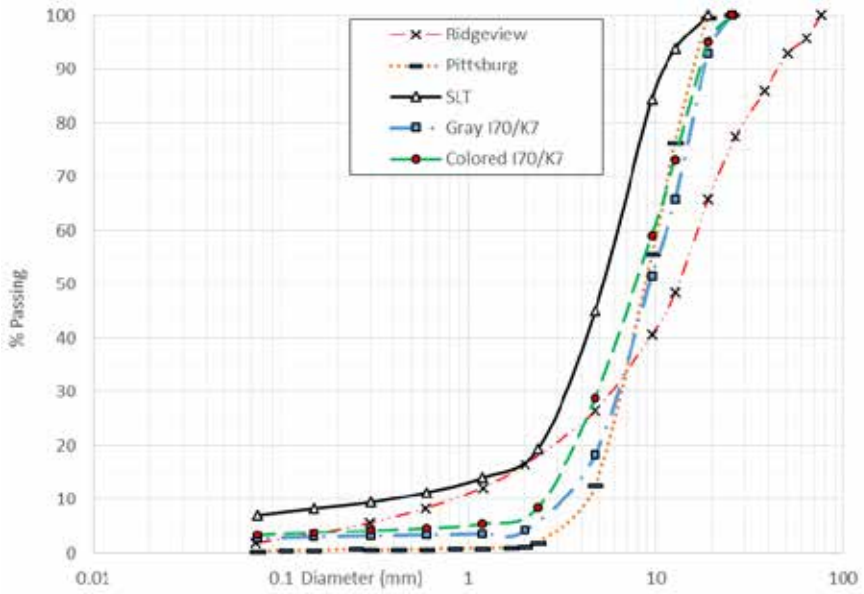

Figure 5.2: Grain Size Distributions of Samples from MSE Walls
Source: Brady et al. (2016)

The GRW5 electrical resistivity showed the widest range because of the low resistivity data beneath the approximate location of the foundation except between 48- 62 ft (14.6- 18.9 m). This wall was constructed where limestone outcrops are prevalent and the resistivity similar to the backfill is likely a rock formation. Additionally, the low resistivity material beneath the foundation is likely the native soil. This material was also used for select fill on top of the wall after construction was complete and the resistivity responses at the surface and below the foundation in Figure 3.18 are similar. As resistivity is a bulk measurement, the low values beneath the footing influence the aggregate measurement at the bottom. Note that while the SLT material is gravel, the sample collected by Brady et al. (2016) contained 7% fine-grained material. This material likely also contributed to the wide range of measured resistivity. Both the lightweight vibratory compactor and the heavy compaction equipment were used at GRW5, causing the variation in measured resistivity near the surface. The confidence interval for GW6 was higher than other structures, however the upper 2 feet (0.59 m) had higher resistivity values than expected and did not appear to be thoroughly compacted at the time of testing. The size of the structure limited compaction equipment to only a vibratory plate compactor.

ERI surveys were conducted on three of the final walls after recent rain events to see the in situ resistivity when water is present. The PDF post-processing of these partially saturated tests (SGW2, SMW4, and SGRW5) are shown in Figure 5.3 along with the original dry survey results. As expected, the measured resistivity data for all partially saturated surveys are lower than the dry surveys. As saturated surveys show the measured resistivity in situ, these results can be used to determine the current minimum resistivity for corrosion potential monitoring. Note that the saturated test of the gravity wall (SGRW5) is only approximately 1,000 Wcm higher than the T 288 sample.

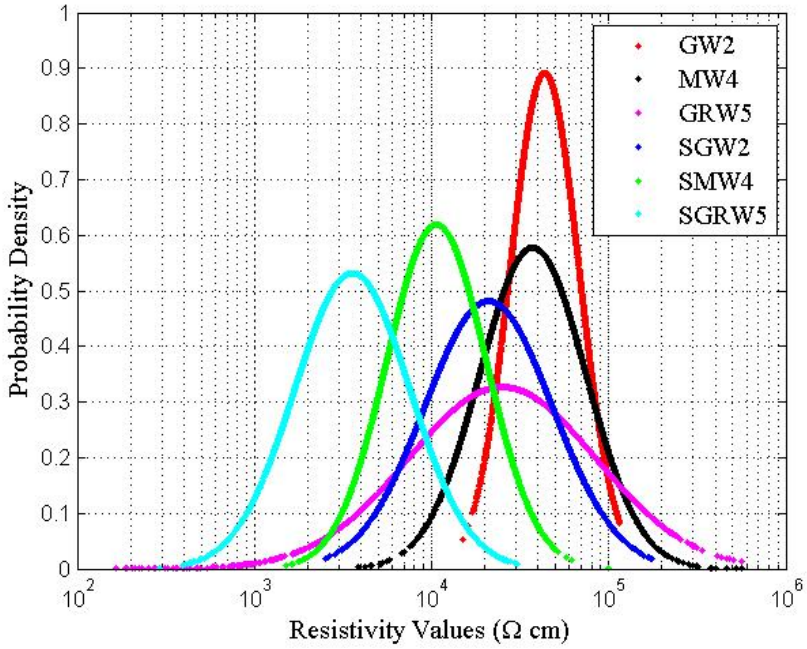

Figure 5.3: Dry and Partially Saturated Survey Bulk Resistivity

One limitation of ERI is the contact between the electrode stakes and the coarse aggregates. As seen at one of the sites, if the backfill aggregate is loosely compacted, the poor contact between the electrodes and the ground will result in a low injection of current and lead to noisy and erroneous electrical resistivity measurements. Geosynthetic Wall 3 aggregate backfill was loosely compacted, producing results significantly higher than the other tested walls (electrical resistivity of approximately 1,000,000 Ohm-cm). ERI must be applied to areas that have recently been compacted to reduce the risk of low quality data.

Results of this study demonstrate ERI is a suitable in situ testing method for measuring bulk electrical resistivity of aggregate backfill of retaining walls. Additionally, ERI has the potential to be used as a monitoring technique for retaining walls due its ability to detect variation within the backfill. Further testing is necessary to understand the effects that reinforcement type, partial water saturation, and compaction have on bulk electrical resistivity of aggregates in order to successfully implement the method for construction monitoring and for determining corrosion potential.

5.1 Comparison with Brady et al. (2016) Laboratory Electrical Resistivity

Only the three partially saturated tests are comparable to the laboratory study by Brady et al. (2016) where material was soaked for 24 hours and allowed to drain freely. The partially saturated tests of GW2, 28,282–30,899 Ωcm, matches the proposed Normal New ASTM results from the Gray I-70/K-7 samples but is lower than the Colored I-70/K-7 results. The partially saturated results from MW4 were 12,737–13,502 Ωcm and higher than the New ASTM Ridgeview; however, the high amounts of fine grained materials affected the New ASTM results. The lower conductivity measurement in the field may similarly be due to the inclusion of fine grained material in the backfill. The influence of metallic reinforcement on ERI needs to be investigated further where fine grained materials are not present because in our experience the reinforcement is possibly too small to influence ERI measurements. Finally, the ERI of the partially saturated GRW5 was 4,533- 4,919 Ωcm, lower than the New ASTM SLT material and the KDOT lower limit. The influence of saturated material at the surface and beneath the foundation likely reduced measured bulk electrical resistivity. Additional partially saturated tests of GRW5 are needed with smaller electrode spacing to reduce the influence of the highly conductive material beneath the structure.

Chapter 6: Recommendations

ERI can be successfully applied to earth retaining structures that are reinforced with metallic or geosynthetic materials or are unreinforced for determining bulk in-place electrical resistivity of the aggregate. The inverted Schlumberger array is recommended due to the shortest testing duration of approximately 35 minutes. The method also provides good vertical resolution when compared to the Wenner and dipole-dipole processes. It is recommended to maximize electrode spacing to image deeper than the wall's height into the native foundation material underneath the wall. However, imaging too much of the native material may alter the results for the aggregates near the base of the wall during the inversion process when native material is highly conductive. This can skew the bulk electrical resistivity calculation as shown in the testing of GRW5. 3D testing is not recommended as the duration of the testing time dramatically increases with minimal extra data gain.

ERI should be done near or at the end of construction. Testing during earlier construction stages provides minimal data, especially for a small retaining wall. Depending on the size of the retaining wall, ERI may require construction to be halted during testing. The effects of continued construction activity, compaction of each layer, and the weight of each additional layer further the compaction and alter the ERI results. If possible, it is recommended that testing be performed when the backfill is known to be dry and also when known to be partially saturated to determine the corrosion potential under different conditions.

Surface compaction influences ERI with higher compaction allowing increased injection of current into the ground and diminished noisy data. Bulk electrical resistivity values decrease with the increase of compaction and vice versa. It is recommended that the survey be run at the end of construction when compaction should be more uniform so the electrical resistivity of the aggregate itself can be determined. The contact resistance test performed prior to any ERI survey is important and should not be ignored. This study determined contact resistance values between 0 and 20,000 Ohm allow enough current into the ground to provide quality data with lower RMS and low noise. Current in between 20,000 to 40,000 Ohm ensures enough current for electrical resistivity measurements, but decreases the accuracy of the results leading to higher RMS,

increase in data noise, and higher electrical resistivity results. Contact resistance results above 40,000 Ohm do not provide enough current to collect reliable data and results are too noisy for interpretation. The more contact between the electrode stake and the gravel, the greater the current supplied to the ground and the more accurate the measurement. Performing electrical resistivity after completion of the retaining wall is advantageous because the native material placed over the aggregates is typically finer-grained, providing better contact, increased injected current, and less noisy and erroneous electrical resistivity measurements. However, few tests were performed in this study after construction, and the testing followed recent rains. More post-construction tests are needed.

Based upon the data gathered during this study, it is recommended that the corrosion potential be reevaluated for coarse aggregates. AASHTO Standard T 288-12 (2012) results are not indicative of coarse aggregates KDOT uses as MSE wall backfill materials. The test requires the soil sample to pass through a No. 10 sieve and a minimum electrical resistivity value be determined which is achieved at saturation. Table 6.1 outlines an update to the corrosion potential for coarse aggregates. Note that no testing was performed in a very corrosive or corrosive environment.

Table 6.1: Corrosion Potential Using ERI

Test Method	**T 288-12**	**Electrical Resistivity Imaging**
Aggressiveness	**Resistivity (Ohm-cm)**	
Very corrosive	<700	Unknown
Corrosive	700 to 2,000	Unknown
Moderately corrosive	2,000 to 5,000	10,000 to 20,000
Mildly corrosive	5,000 to 10,000	20,000 to 40,000
Noncorrosive	>10,000	>40,000

6.1 Future Work

Additional ERI testing of MSE walls with varying types of reinforcement is needed to further define the effects of reinforcement. Only one wall containing metallic reinforcement was available for testing in this study. The other MSE walls were reinforced with geosynthetics, which appeared to have no effect to the results as compared to an unreinforced structure. Similarly, testing of aggregates that are thought to be corrosive is needed. The walls tested in this study had many different compaction methods which affected the electrical resistivity results. More testing in a controlled environment with varying types of compaction equipment and measured in situ density are required to further define the correlation that exists between compaction and electrical resistivity. ERI was also performed after and during rain events with water known to be present within the backfill, lowering electrical resistivity results. It is advised that further testing be completed to fully understand the correlation of degree of saturation and water chemistry to electrical resistivity and corrosion potential.

Based upon the results from this particular study, compaction, varying types of reinforcement (metallic and geosynthetic), partial water saturation, and water chemistry should be analyzed to determine their effect in a controlled laboratory setting. Material other than coarse aggregates should also be tested as these materials would produce different results than those seen in this study. Additionally, materials that are known to be highly corrosive should be tested. ERI has the potential to be used as a monitoring technique for not only retaining wall structures, but also for other buried infrastructure, such as pipes.

References

AASHTO Standard T 288-12. (2012). *Standard method of test for determining minimum laboratory soil resistivity*. Washington, DC: American Association of State Highway and Transportation Officials.

Advanced Geosciences, Inc. (AGI). (2007). *Instruction manual for EarthImager 2D Resistivity and IP Inversion Software*. Austin, TX: Author.

Arjwech, R., Everett, M.E., Briaud, J.-L., Hurlebaus, S., Medina-Cetina, Z., Tucker, S., & Yousefpour, N. (2013). Electrical resistivity imaging of unknown bridge foundations. *Near Surface Geophysics*, *11*(6), 591-598.

Armour, T., Bickford, J., & Pfister, T. (2004). Repair of failing MSE railroad bridge abutment. In J.P. Turner & P.W. Mayne (Eds.), *GeoSupport 2004: Drilled Shafts, Micropiling, Deep Mixing, Remedial Methods, and Specialty Foundation Systems* (pp. 380-394). Reston, VA: American Society of Civil Engineers.

ASTM G57-06. (2006). *Standard test method for field measurement of soil resistivity using the Wenner four-electrode method*. West Conshohocken, PA: ASTM International. doi: 10.1520/G0057-06, www.astm.org

ASTM G187-12a. (2012). *Standard test method for measurement of soil resistivity using the two-electrode soil box method*. West Conshohocken, PA: ASTM International. doi: 10.1520/G0187-12A, www.astm.org

Baecher, G.B., & Christian, J.T. (2005). *Reliability and statistics in geotechnical engineering*. Hoboken, NJ: John Wiley & Sons.

Bai, W., Kong, L., & Guo, A. (2013). Effects of physical properties on electrical conductivity of compacted lateritic soil. *Journal of Rock Mechanics and Geotechnical Engineering*, *5*(5), 406-411.

Berg, R.R., Christopher, B.R., & Samtani, N.C. (2009a). *Design of mechanically stabilized earth walls and reinforced soil slopes – Volume I* (Report No. FHWA-NHI-10-024). Washington, DC: Federal Highway Administration.

Berg, R.R., Christopher, B.R., & Samtani, N.C. (2009b). *Design of mechanically stabilized earth walls and reinforced soil slopes – Volume II* (Report No. FHWA-NHI-10-025). Washington, DC: Federal Highway Administration.

Bernstone, C., Dahlin, T., Ohlsson, T., & Hogland, W. (2000). DC-resistivity mapping of internal landfill structures: Two pre-excavation surveys. *Environmental Geology, 39*(3-4), 360-371.

Brady, Z., Parsons, R., & Han, J. (2016). *Testing aggregate backfill for corrosion potential* (Report No. K-TRAN: KU-15-5). Topeka, KS: Kansas Department of Transportation.

Chambers, J.E., Wilkinson, P.B., Penn, S., Meldrum, P.I., Kuras, O., Loke, M.H., & Gunn, D.A. (2013). River terrace sand and gravel deposit reserve estimation using three-dimensional electrical resistivity tomography for bedrock surface detection. *Journal of Applied Geophysics, 93*, 25-32.

Devore, J.L. (2004). *Probability and statistics for engineering and sciences* (6th ed.). Belmont, CA: Brooks/Cole–Thomson Learning.

Edwards, L.S. (1977). A modified pseudosection for resistivity and IP. *Geophysics, 42*(5), 1020-1036.

Elias, V., Fishman, K.L., Christopher, B.R., & Berg, R.R. (2009). *Corrosion/degradation of soil reinforcements for mechanically stabilized earth walls and reinforced soil slopes* (Report No. FHWA-NHI-09-087). Washington, DC: Federal Highway Administration.

Everett, M.E. (2013). *Near-surface applied geophysics*. Cambridge, UK: Cambridge University Press.

Federal Highway Administration (FHWA). (2015). *Geotechnical engineering*. Retrieved from http://www.fhwa.dot.gov/engineering/geotech/

Furman, A., Ferré, T.P., & Warrick, A.W. (2003). A sensitivity analysis of electrical resistivity tomography array types using analytical element modeling. *Vadose Zone Journal, 2*(3), 416-423.

Hallof, P.G. (1957). *On the interpretation of resistivity and induced polarization field measurements* (Doctoral dissertation). Massachusetts Institute of Technology, Cambridge, MA.

Kansas Department of Transportation (KDOT). (2007). *KDOT Geotechnical Manual*. Retrieved from https://www.ksdot.org/descons.asp

Loke, M.H. (1999). *Electrical imaging surveys for environmental and engineering studies—A practical guide to 2-D and 3-D surveys* [Notes]. Minden Heights, Malaysia.

Lowrie, W. (2007). Earth's age, thermal and electrical properties. In *Fundamentals of geophysics* (2nd ed., pp. 207-280). Cambridge, UK: Cambridge University Press.

Stummer, P., Maurer, H., & Green, A.G. (2004). Experimental design: Electrical resistivity data sets that provide optimum subsurface information. *Geophysics, 69*(1), 120-139.

Thapalia, A., Borrok, D., Nazarian, S., & Garibay, J. (2011). Assessment of corrosion potential of coarse backfill aggregates for mechanically stabilized earth walls. *Transportation Research Record, 2253*, 63-72.

Thornley, J.D., & Siddharthan, R.V. (2010). Effects of corrosion aggressiveness on MSE wall stability in Nevada. In R. Finno, Y. Hashash, & P. Arduino (Eds.), *Earth Retention Conference 3: Proceedings of the 2010 Earth Retention Conference* (pp. 539-547). Reston, VA: American Society of Civil Engineers.

Tucker, S., Briaud, J., Hurlebaus, S., Everett, M., & Arjwech, R. (2015). Electrical resistivity and induced polarization imaging for unknown bridge foundations. *Journal of Geotechnical and Geoenvironmental Engineering, 141*(5). doi: 10.1061/(ASCE)GT.1943-5606.0001268

Vaudelet, P., Schmutz, M., Pessel, M., Franceschi, M., Guérin, R., Atteia, O.,… Bégassat, P. (2011). Mapping of contaminant plumes with geoelectrical methods. A case study in urban context. *Journal of Applied Geophysics, 75*(4), 738-751.

Zhou, Q.Y., Shimada, J., & Sato, A. (2001). Three-dimensional spatial and temporal monitoring of soil water content using electrical resistivity tomography. *Water Resources Research, 37*(2), 273-285.

Zonge, K., Wynn, J., & Urquhart, S. (2005). Resistivity, induced polarization, and complex resistivity. In D.K. Butler (Ed.), *Near-surface geophysics* (pp. 265-300). Tulsa, OK: Society of Exploration Geophysicists.

Appendix A: Preliminary ERI Post Processing

GW1 histogram and PDF shown in Figure 3.19 and Figure 3.20.

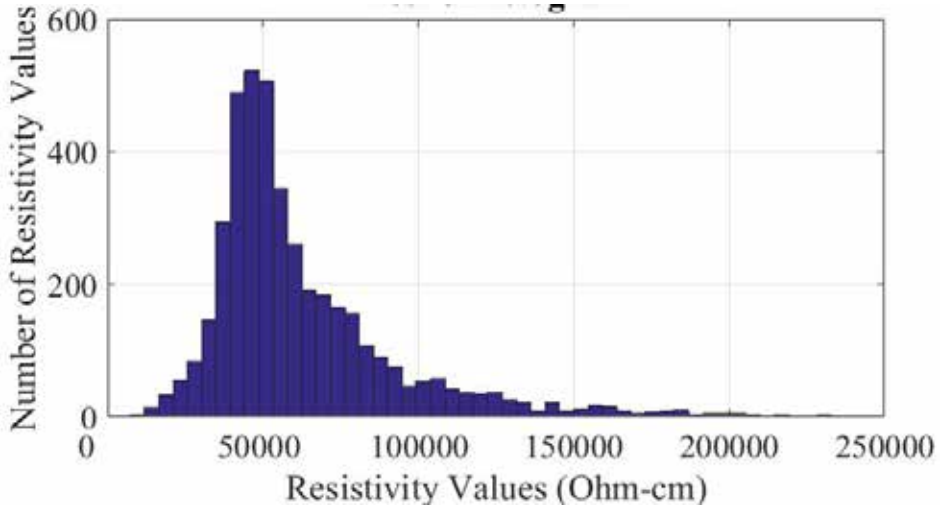

Figure A.1: GW2 Histogram

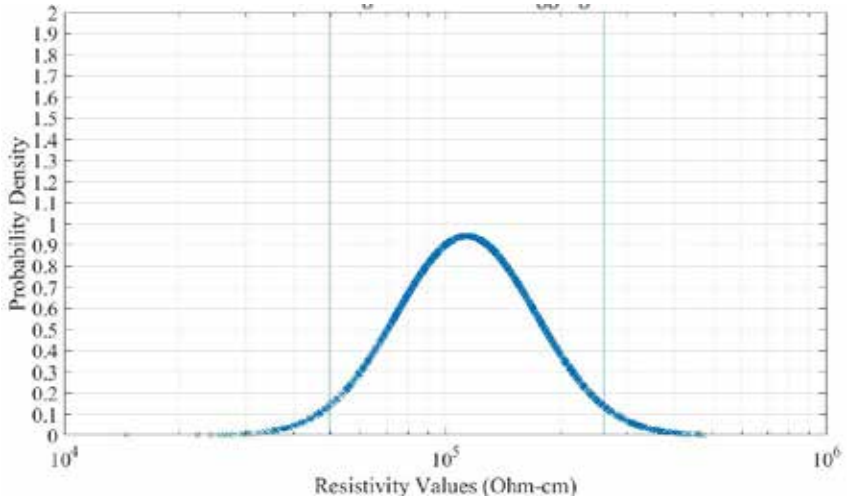

Figure A.2: GW2 PDF

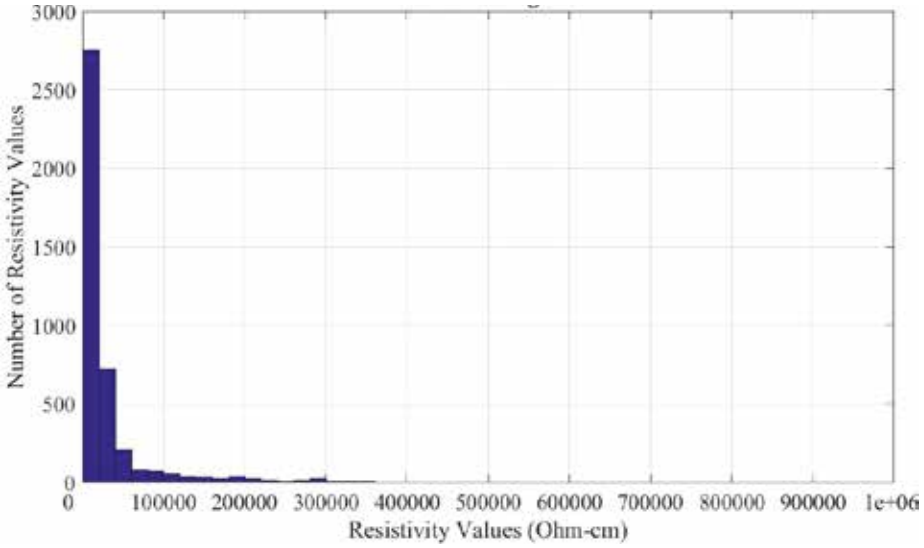

Figure A.3: MW4 Histogram

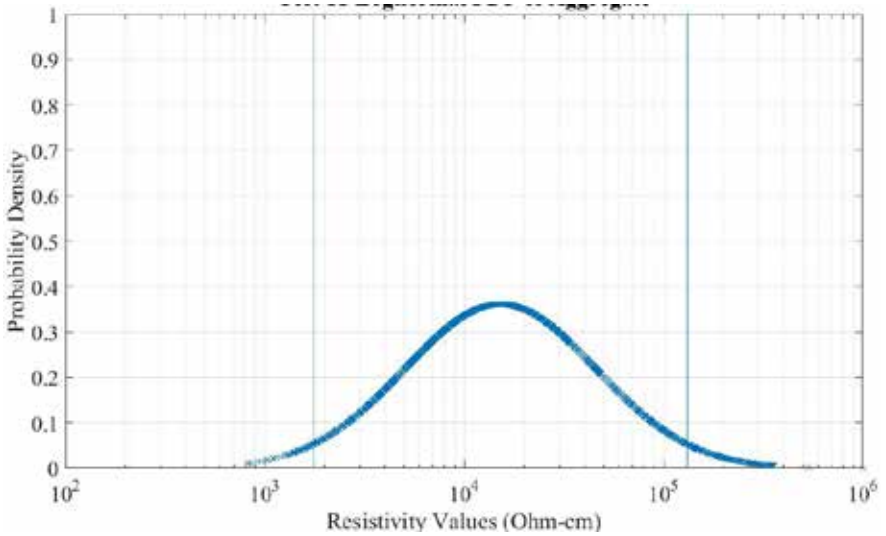

Figure A.4: MW4 PDF

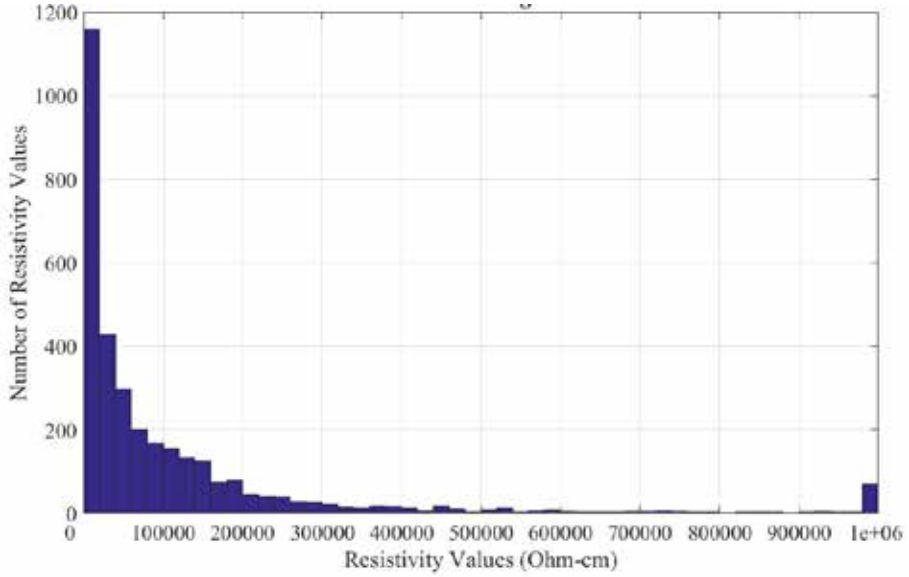

Figure A.5: GRW5 Histogram

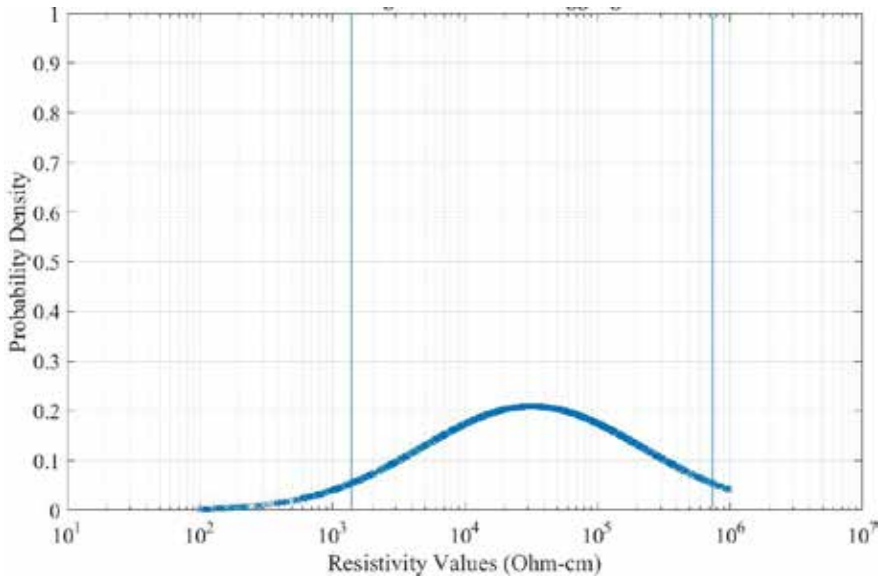

Figure A.6: GRW5 PDF

Appendix B: Partially Saturated Post Processing

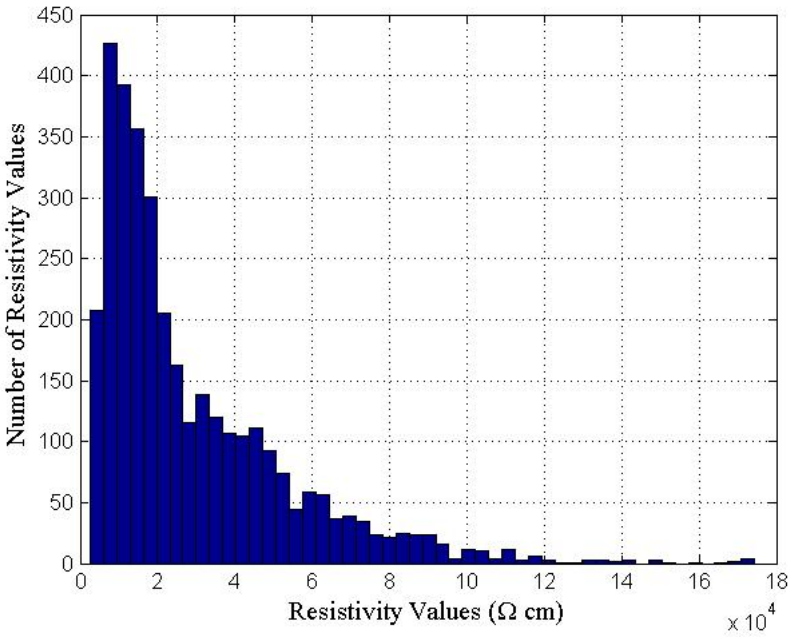

Figure B.1: SGW2 Histogram

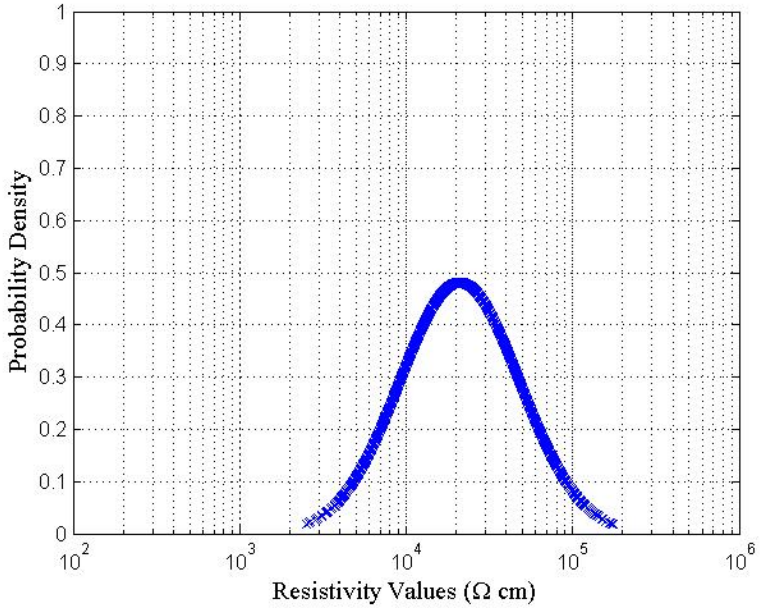

Figure B.2: SGW2 PDF

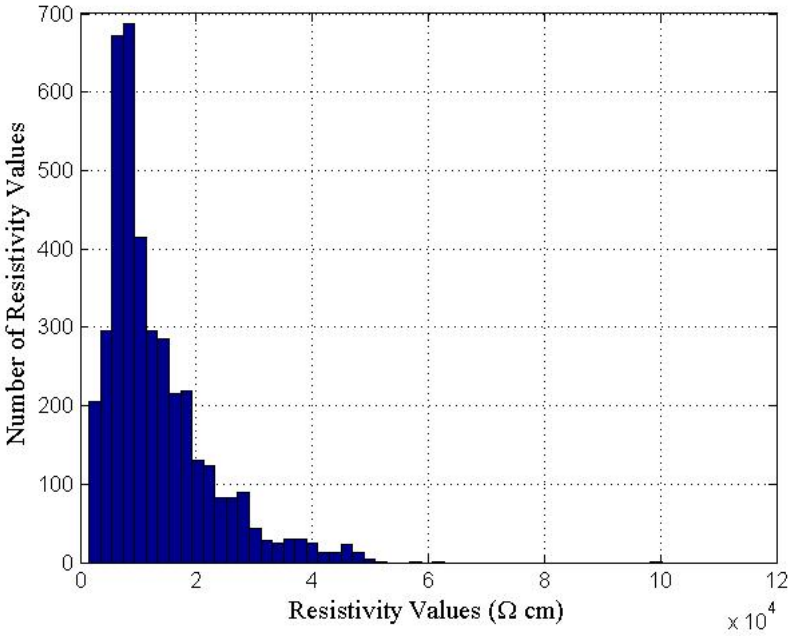

Figure B.3: SMW4 Histogram

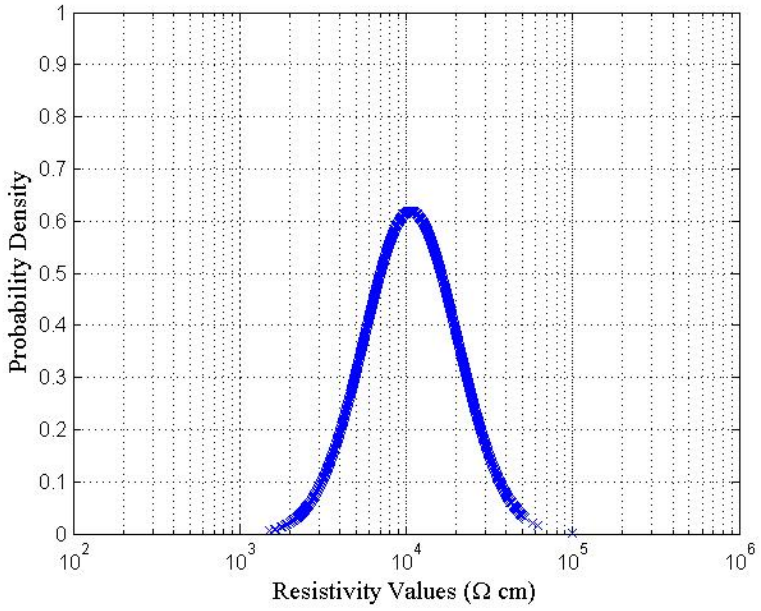

Figure B.4: SMW4 PDF

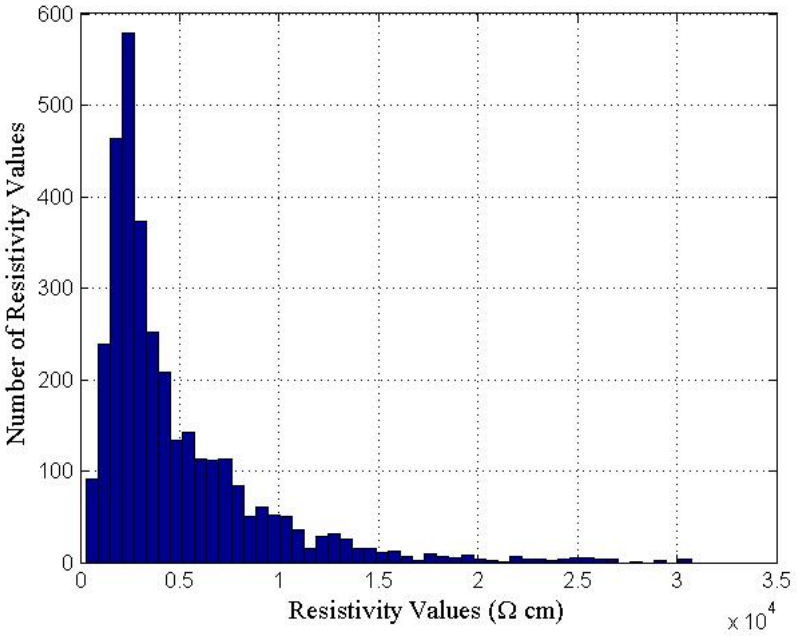

Figure B.5: SGR5 Histogram

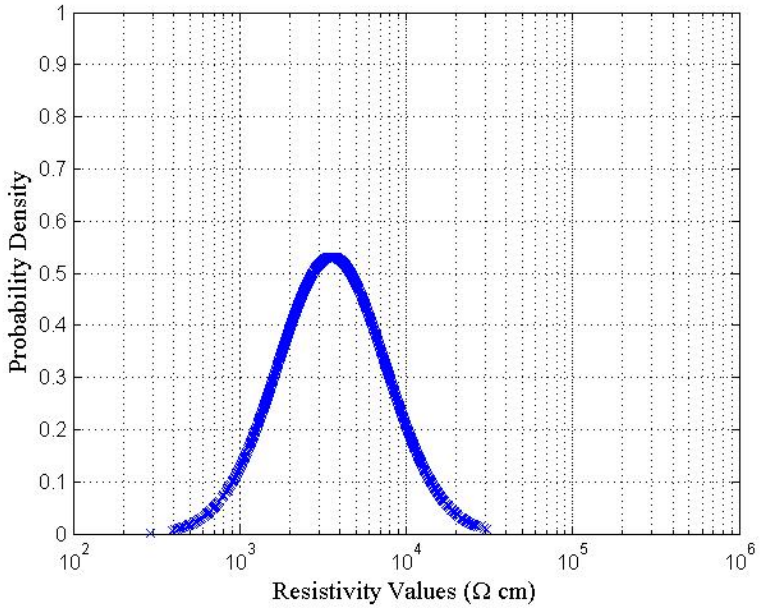

Figure B.6: SGR5 PDF

K-TRAN

KANSAS TRANSPORTATION RESEARCH AND NEW-DEVELOPMENT PROGRAM

AD ASTRA PER ASPERA

Kansas

Department of Transportation